

8-8-2011

A STUDY OF THE LHIRES III SPECTROGRAPH ON THE HARD LABOR CREEK OBSERVATORY 20 INCH TELESCOPE

Benjamin G. Jenkins

Georgia State University, jenkins@chara.gsu.edu

Recommended Citation

Jenkins, Benjamin G., "A STUDY OF THE LHIRES III SPECTROGRAPH ON THE HARD LABOR CREEK OBSERVATORY 20 INCH TELESCOPE" (2011). *Physics and Astronomy Theses*. Paper 12.
http://digitalarchive.gsu.edu/phy_astr_theses/12

This Thesis is brought to you for free and open access by the Department of Physics and Astronomy at Digital Archive @ GSU. It has been accepted for inclusion in Physics and Astronomy Theses by an authorized administrator of Digital Archive @ GSU. For more information, please contact digitalarchive@gsu.edu.

A STUDY OF THE LHIRES III SPECTROGRAPH ON THE HARD LABOR CREEK
OBSERVATORY 20 INCH TELESCOPE

by

BENJAMIN G. JENKINS

Under the direction of Douglas Gies

ABSTRACT

I present a study done to determine the characteristics of the LHIRES III spectrograph on the 20 inch RC Optics telescope at Hard Labor Creek Observatory. I describe the settings of three different diffraction gratings, collimation and focus issues, and practical aspects of use. The spectrograph was used with a SBIG ST-8XME camera for all studies. Data collection was accomplished with the Maxim DL software package and analysis was completed with IRAF. Solutions for the dispersion relation with all three diffraction gratings were found. Several projects are underway with this instrument. I present time series spectra of α Vir to demonstrate the practical applications of the spectrograph. This non-radially pulsating star shows Doppler shifts that were recorded in the Si III 4552, 4568, 4574 Å triplet over the course of a night. The observed profile variations showed the spectrograph capable of exacting scientific work.

INDEX WORDS: Spectra, Gratings, Spectrograph, LHIRES III, α Vir

A STUDY OF THE LHIRES III SPECTROGRAPH ON THE HARD LABOR CREEK
OBSERVATORY 20 INCH TELESCOPE

by

BENJAMIN G. JENKINS

A Thesis Submitted in Partial Fulfillment of the Requirements for the Degree of

Master of Science

in the College of Arts and Sciences

Georgia State University

2011

Copyright by
Benjamin Gordon Jenkins
2011

A STUDY OF THE LHIRES III SPECTROGRAPH ON THE HARD LABOR CREEK
OBSERVATORY 20 INCH TELESCOPE

by

BENJAMIN G. JENKINS

Committee Chair: Douglas Gies

Committee: Michael Crenshaw

Russel White

Electronic Version Approved:

Office of Graduate Studies

College of Arts and Sciences

Georgia State University

August 2011

DEDICATION

This work is dedicated to my daughter Felicity Lark and to my wife Katelyn. This work would not have been possible without their positive influence on my life.

ACKNOWLEDGEMENTS

It is within these next few pages that I am to thank everyone who assisted in some way, shape, or form in the completion of this work. To that end I first wish to thank Nic Scott and Noel Richardson. Nic and Noel were greatly involved in the instrumentation setup of the telescope and the mount. Nic in addition was the first person to work with the spectrograph and get spectra through it. He was a great help in the infancy of the project and is still involved when something goes wrong.

Also great thanks to Noel Richardson and Emily Aldoretta. Both of them were in the dome on the first night that we obtained spectra, and they have been of great help in collecting extra data and in making additional tests, that, because of time constraints, I could not properly obtain myself. Noel in particular was extremely helpful by giving me a crash course in data reduction in IRAF.

Another person to whom I owe gratitude is Olivier Thizy of Shelyak Instruments. When I was unable to find specific information, Mr. Thizy responded by email to my queries the next day and with far more information than I had hoped to receive. Because of his assistance I am able to include several graphs concerning the blaze efficiencies of the gratings.

I would also like to thank Dr. Richard Miller. I have now completed my “work of fiction” as he once jokingly called this paper. It is hardly a fiction, though in the long hours spent working on the transcript, it did at times seem as though I had fallen through the computer screen, and I had my share of “off with his head!” moments as revelations came to light concerning the data I had collected. These prompted several rushed trips to Hard Labor Creek Observatory (HLCO), much to my wife’s chagrin. I have worked with Dr. Miller on trying to accommodate my strange schedule and finish the program at Georgia State University (GSU) in enough time to fulfill my

family obligations. He has worked with me in many ways to make certain that I had both a full workload and the opportunity to finish with my research in a timeframe that was in my best interests. For this I am grateful. I also need to thank him for acquiring the lovely instruments which I have had the pleasure of working with over the past few months. It is simply amazing to get to work with such fine tools that he has managed to provide for the department.

I am also deeply indebted to Dr. Douglas Gies for all of his great insights and assistance with both my scheduling and my academics. When I first arrived at GSU and explained to him that I would need to have a slightly compressed timeline, i.e., finish my Master's Program in a year, he immediately set about thinking of ways which would allow me to accomplish that goal. It was under his advisement I began working with the LHIRES III spectrograph and spectroscopy in general. Having worked in the field of spectroscopy since well before my birth, he has been a wonderful mentor at each step, and it is a great privilege to work under him. Much of the work in this thesis could not have been done without his vast knowledge of the various methods of how to manipulate spectra and his willingness to aid me along the way.

I also owe thanks to Dr. Bob Powell, and Robert Moore Jr. of the University of West Georgia (UWG). Dr. Powell was my undergraduate advisor and of great assistance to my application and acceptance to GSU. It was under his tutelage that I became certain that astronomy was the interest to which I wish to devote the rest of my time, and his offers to use resources of UWG, while sadly rejected due to the nature of my research, are still warmly received. Mr. Moore provided me with both rides to and from HLCO and a perfect backboard for bouncing ideas and problems off of, as well as providing the best understanding of the imaging software Maxim DL. Of the many people I worked with in my research. I believe that he, more than any, started me on the path of my love of all things astronomy.

And finally I owe great thanks to all of my family members. To both my parents and my in-laws for the great assistance that they gave to my wife and I in watching our daughter and the moral support they provided as we finished our schooling and started our own life together. To my wife, who, while not understanding everything I needed to do, or the field of astronomy in general, stuck by my side and gave me the time I needed to finish my work. And to my daughter for reminding me that occasionally I need to stop working and play every now and then, regardless of how much I love my work, as well as for giving me the reason I needed to continue when the work did not seem worth the prize.

Benjamin G. Jenkins

June 6th, 2011

TABLE OF CONTENTS

ACKNOWLEDGEMENTS	v
LIST OF TABLES	x
LIST OF FIGURES	xi
1. INTRODUCTION	1
2. THE EQUIPMENT	3
2.1 The Telescope	3
2.2 The Spectrograph	6
2.2.1 The Slit	10
2.2.2 Guide Camera	13
2.2.3 The Neon Comparison Lamp	15
2.2.4 The Main Mirror and Collimator Focus	15
2.2.5 The Gratings	20
2.3 The CCD	36
3. REDUCING THE DATA	40
4. RESULTS	46
5. OBSERVATIONS OF α Vir = HD 116658	51
6. CONCLUSIONS	57
References	59
Appendix	60
A. Users Guide	60
A.1 Telescope Start-Up	60
A.2 Using the Spectrograph	61

A.2.1. To Connect the ST-8 to the Computer	61
A.2.2. Maxim DL	62
A.2.3. Guide Camera	62
A.3. Prior to Observing	64
A.4. Observing Procedure	70
A.5 Closing Down	74
B. Atlas of Neon Lines	77

LIST OF TABLES

Table 2.1: Angular Size of Slit upon the Sky.	12
Table 2.2: The Gratings and their Respective Blaze Angles.	20
Table 2.3: 2400 g/mm Grating Data.	31
Table 2.4: 600 g/mm Grating Data.	32
Table 2.5: 150 g/mm Grating Data.	33
Table 5.1: Radial Velocity of α Vir Line Profiles.	56
Table B.1 Known Ne Lines.	75

LIST OF FIGURES

Figure 2.1: The Optical Path of the LHIRES III.	8
Figure 2.2: A view of the HLCO 20 inch telescope and spectrograph.	9
Figure 2.3: The highly polished slit plate.	11
Figure 2.4: The Slit Access panel on the Spectrograph.	14
Figure 2.5: The Main Mirror Adjustment Screw.	17
Figure 2.6: The Collimation Access Panel.	18
Figure 2.7: The Collimator.	19
Figure 2.8: Adjusting the Collimator.	19
Figure 2.9: The blaze efficiency for the 150 g/mm grating.	21
Figure 2.10: The blaze efficiency for the 600 g/mm grating.	22
Figure 2.11: The blaze efficiency for the 2400 g/mm grating.	23
Figure 2.12: An image of the grating mount.	24
Figure 2.13: Mechanical Interior of the LHIRES III.	27
Figure 2.14: Micrometer position vs. $\sin \beta$.	28
Figure 2.15: Micrometer position vs. Wavelength.	30
Figure 2.16: Example of Orders Blending.	35
Figure 2.17: Quantum Efficiency of the ST-8XME.	37
Figure 2.18: Linearity of the ST-8.	38
Figure 2.19: ST-8 Hot Pixels.	39
Figure 3.1: Wavelength Calibration.	43
Figure 3.2: Calibration Variation.	45
Figure 4.1: A Sample Spectrum using the 2400 g/mm Grating	49

Figure 4.2: Spectra of Deneb.	50
Figure 5.1: Average Spectrum of α Vir.	53
Figure 5.2: Line Profile Variability of α Vir.	54
Figure 5.3: Radial Velocity of Line Profile Variability.	55
Figure A.1: A View of the Camera Positions.	64
Figure A.2: Neon lamp configuration.	67
Figure A.3: Collimator access panel.	68
Figure A.4: Collimator adjustment.	69
Figure A.5: The Main Mirror Adjustment Screw.	70

1. INTRODUCTION

When I first arrived at Georgia State University in 2010, the Department of Physics and Astronomy had just finished the rough installation of its new 20 inch RC Optical telescope at its Hard Labor Creek Observatory (HLCO). HLCO is used for instrument development, astronomical observations, public open house nights, and by GSU students in the introductory level astronomy courses to fulfill a requirement to visit an observatory. Students visit, view, and then write a report on various celestial objects as well as the telescopes used for viewing. In the past the observatory was used for research utilizing the Multiple Telescope Telescope (MTT), a 16 inch Meade telescope, and a 16 inch Boller & Chivens telescope. With the installation of the 20 inch, the beginning of a new wave of research was promised. Issues of fine alignment and troubleshooting with the mounting and software kept the telescope from being used for research until recently.

Once the issues with the 20 inch RC telescope were resolved, the next step was to obtain light for use in scientific endeavors. And so on the night of UT 2011 May 5 first light was passed through the LHIRES III spectrograph and the first images were recorded which could be used for scientific research. It was quite a feat considering that the telescope had been undergoing troubleshooting for well over eight months at that point. There was a palpable sense of relief in the dome that science could be done with our newest setup.

Now we needed to determine how much science could be done. An understanding of the spectrograph, observing procedure, and the data reduction processes were also needed. Once established these would need to be documented to be passed along to the next wave of researchers who would use the spectrograph. This is where I entered the fray. After spending hours running the telescope and spectrograph and working with the data, I present to the reader

my understanding of the instruments. I offer the best procedures to follow to achieve the least headache and most productivity.

Section 2 describes the telescope and the mount along with the spectrograph. Especially useful to the observer will be Section 2.2. Section 2.2.1 describes the slit and how to change it, as well as its angular size on the sky. Section 2.2.5 is likely the most useful section with information about the micrometer relation to wavelength, the dispersion relations, and resolution of all gratings. Section 3 has information about data reduction, and a few tricks to use when wavelength calibration becomes difficult. Sections 4 and 5 show results from early, currently ongoing research, including results on Deneb and α Vir. A user's guide is presented in Appendix A, and it is my hope that this guide will be used to help future researchers through the labyrinth of obtaining useful images. Appendix B lists the available neon lines that are used for wavelength calibration.

A plethora of wishes and desires for streamlining the entire setup and increasing productivity along with the simple hopes for retrieval of better data will also be presented within the pages of text which follow here. It is likely that after reading the entirety of this work, one will still come away with questions that will only be answered by personal experience. But then if that were not the case, where would the challenge and fun in life be?

2. THE EQUIPMENT

2.1 The Telescope

The primary research telescope at HLCO is currently the RC Optical 20 inch telescope. The optical design is a Ritchey-Chrétien. This design has two reflecting surfaces, as well as no refracting element in the path until one reaches the eyepiece or instrument mounted upon the back of the telescope. This makes the telescope color insensitive as there is no chromatic aberration from refraction, and it also allows for high light throughput. Another aspect of the RC design is that the curvatures of the mirrors are both hyperbolic. This feature results in reduced coma when compared to other styles of telescopes, specifically the Schmidt-Cassegrain and Cassegrain designs.

The telescope has a focal ratio of $f/8.1$, with a manufacturer certified optical surface better than $1/20^{\text{th}}$ wave rms.¹ The mirrors are coated with SiO₂ and TiO₂ layers that lead to a reflectivity of 96.9%. On board coolers can be utilized to cool the primary mirror to ambient temperature. The telescope structure is a low-expansion carbon fiber truss. The telescope is focused with the secondary mirror, and back focus is adjusted by adding or removing threaded rings to the eyepiece mount.

This instrument is set on an Astro-Physics 3600GTO “el Capitan” German equatorial mount. The mount is one of the premier mounts manufactured by Astro-Physics for large telescopes that are used primarily for imaging.² The telescope is driven by highly accurate motors that have a known step size of 0.05 arcsec/step according to the manufacturer claims. The mount has ability to track past the meridian, which is especially important, because German equatorial mounts are notorious for the requirement that at the meridian they must slew the north-south by axis 180

¹ For more information visit <http://www.rcopticalsystems.com/>.

² For more information visit <http://www.astro-physics.com/index.htm?products/mounts/3600gto/3600gto>.

degrees before resuming tracking. The 3600GTO's ability to ignore this flip while tracking any object is useful. However, it is important to note that if one slews to a different object on the other side of the meridian then the telescope axis will have to undergo the 180 degree flip about the north-south axis.

The current method for controlling the telescope is an on-site computer which is situated within the dome alongside the telescope itself. The mount can be operated by the computer programs which come with the telescope or by "The Sky" (Software Bisque) for ease of pointing and slewing.³ All systems for the mount will eventually be run through on-site computers, however, our current situation is such that the integral hand panel and target list for the mount are the main source for slewing and pointing. Once the target is acquired there is drift of approximately 1 arc second per minute, if no guide camera is operating.

Controls for focusing and minor pointing corrections are relayed through the on-site computers. The Pulse Guide v1.37 program is used with the guide camera provided with the spectrograph to do fine guiding manually. There are a few problems with this set up and some changes that we would like to make.

First it takes some time on the part of the user to become accustomed to the directions in the guide camera, and which direction button they correspond to in Pulse Guide, the software box for guiding. These directional elements will also change depending upon the position of various objects in the sky and the telescope's position east or west of the polar axis. Our current system of mounting the spectrograph to the telescope resulted in a slit orientation about 30° from an east-west alignment. A threaded plate fastened to the spectrograph is screwed into eyepiece spacers at the rear of the telescope until tight. Because there are six screws which attach this

³ For more information concerning "The Sky" visit the Software Bisque website at <http://www.bisque.com/sc/pages/thesky6family.aspx>.

plate to the spectrograph we have six choices for slit orientation upon the sky, at discreet 60° intervals. The ability to set the slit image at a particular angle is useful in the case of atmospheric dispersion. By orienting the slit along the great circle from zenith to the horizon the effects from this dispersion can be removed. This limitation will hopefully be addressed by an improved system of attaching and detaching instruments to the telescope.

Secondly we would like to find some method of auto guiding to keep objects upon the same point of the slit for extended exposures, so that one is not required to check upon the guiding continually. A better guide camera and some more advanced software will likely be needed for this step. Lastly there is hope for a better system for locating the slit in the guide camera field of view. It is easy to locate the slit, either during daylight hours or by turning on lights in the dome to illuminate the slit at night. Once the slit can be seen, a sticky note is applied to the computer screen along the slit. When it is dark and the slit is difficult to see, the telescope can be moved to place the object on the corner of this sticky note to ensure that it is located upon the slit. While low tech, this procedure has successfully, if temporarily, solved the issues of finding the slit and placing the object upon it for manual fine guiding. This problem will likely be solved with a better guide camera and the introduction of guider software.

Once the final issues relating to the slewing of the telescope are resolved, the control computer will be moved into the electronics room adjacent to the dome. There are numerous issues with having the control center set in the same room as our equipment, including the introduction of stray light and heat. To combat some of these problems, the computers are run in a “night mode” where the desktop and all programs are run in a red color format. There is also a small desk lamp with a red bulb to help preserve night vision of the observers and reduce the

amount of ambient light in the dome. This has introduced problems for red wavelength spectroscopy. Removing the computers from the dome will resolve these worries.

2.2 The Spectrograph

The LHIRES III spectrograph is an instrument first envisioned in 2003 as a tool for use by amateur astronomers.⁴ LHIRES III stands for Littrow HI REsolution Spectrograph, and it is the third and final design, which was completed by its designer, Christian Buil, in 2005. The goal for an inexpensive, yet powerful and high resolution spectrograph came about at a conference in Oléron, France, where work presented by amateur astronomers showed the many uses of a high resolution, cheap spectrograph. The specifications for the LHIRES III were that it have a resolving power, $\lambda/\Delta\lambda$ of $R \geq 10,000$, and that it be a solid instrument capable of being mounted to a 8 inch f/10 telescope. The LHIRES III has met these requirements and is now in production by Shelyak Instruments.

The design is based upon a Littrow type reflecting spectrograph, and with the default 2400 grooves/mm grating the manufacture's claim is that a resolving power of $R=17,000$ is achieved. The manufacturer further claims that with telescope apertures in the range of 8-16 inches the limiting magnitude range is between 6 and 8. We discuss below the different diffraction gratings and their limiting magnitudes as well as their dispersions and spectral ranges. Many of the manufacturer specifications have held true for our own set up, although our limiting magnitude, $V = 8.5$, is set by the current guide camera rather than limits imposed by the spectrograph itself.

This Littrow spectrograph is made with a lens that serves as the collimator and the camera as well. This helps to minimize the size of the spectrograph. Littrow's are also characterized by having the angle of incidence and the angle of diffraction nearly equal. All of this equates to a

⁴ See the manufactures web site for more details about the LHIRES III.
<http://www.astrosurf.com/thizy/lhires3/index-en.html>.

powerful high resolution instrument which can be contained in a small space. To visualize the optical path see Figure 2.1. The light enters the spectrograph via the telescope. It is brought to focus at the slit. Some of the light is transmitted back to a mirror which sends light to a slit viewing camera for guidance purposes. The light passing through the slit hits a 45° principal mirror and is sent to the collimator. There it is collimated and proceeds as parallel light rays to the grating. It hits the grating and is diffracted, then is returned nearly along the same path. The returning light hits the collimator, which now functions as a camera, and the light is finally focused at the CCD detector.

There are several parts to this spectrograph that need to be adjusted by the observer before taking any images through the spectrograph. Appendix A is the user guide that will be provided to all users of the spectrograph at HLCO. It will give detailed instruction about the practical aspects of the adjustments and the order in which they need to be made. Here I will make note of the parts, their function, and their adjustment. A picture of our set up can be seen in Figure 2.2.

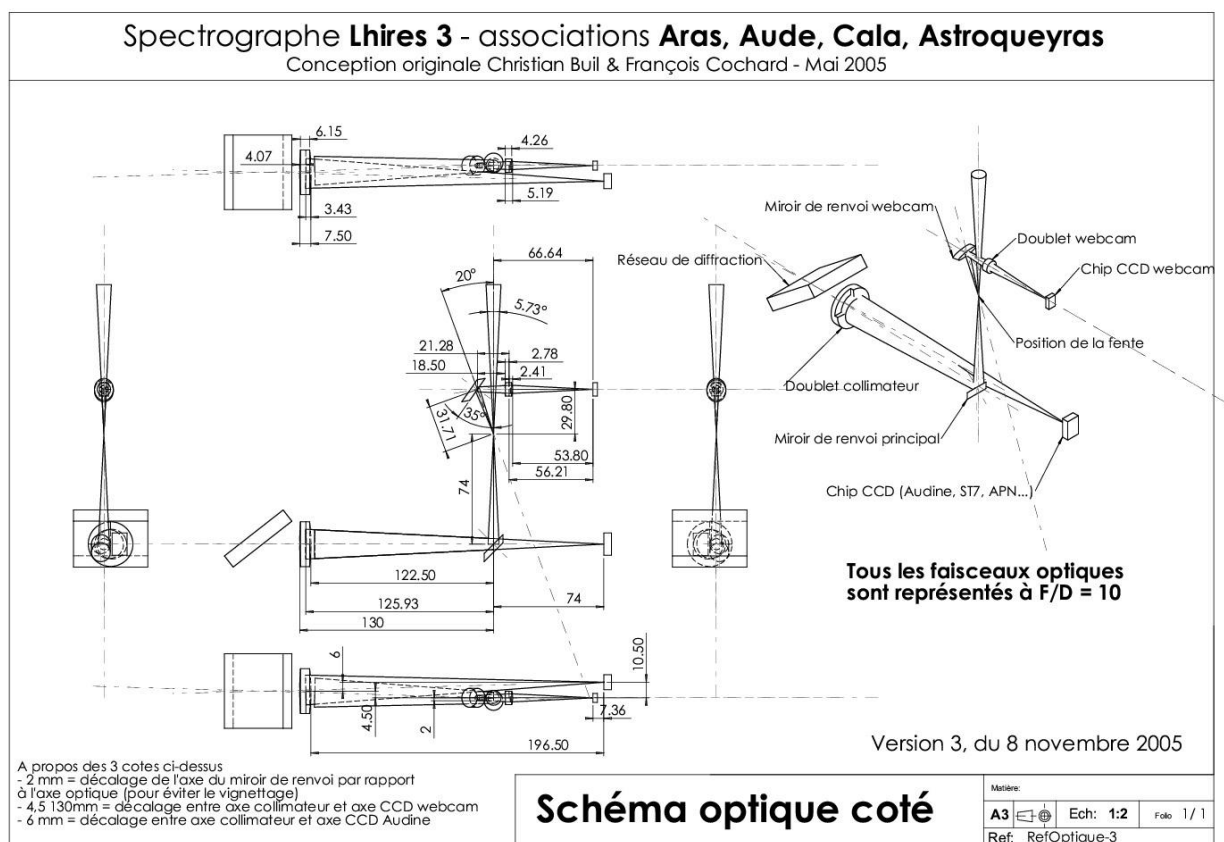


Figure 2.1: The Optical Path of the LHIRES III. This schematic of the interior of the LHIRES III shows the basic outlay of all optical components from several angles. The light enters via the telescope and is brought to focus at the slit. As it can be seen the doublet serves as a collimator and a camera. *Image found at manufacturer's website, <http://www.astrosurf.com/thizy/lhires3/index-en.html>.*

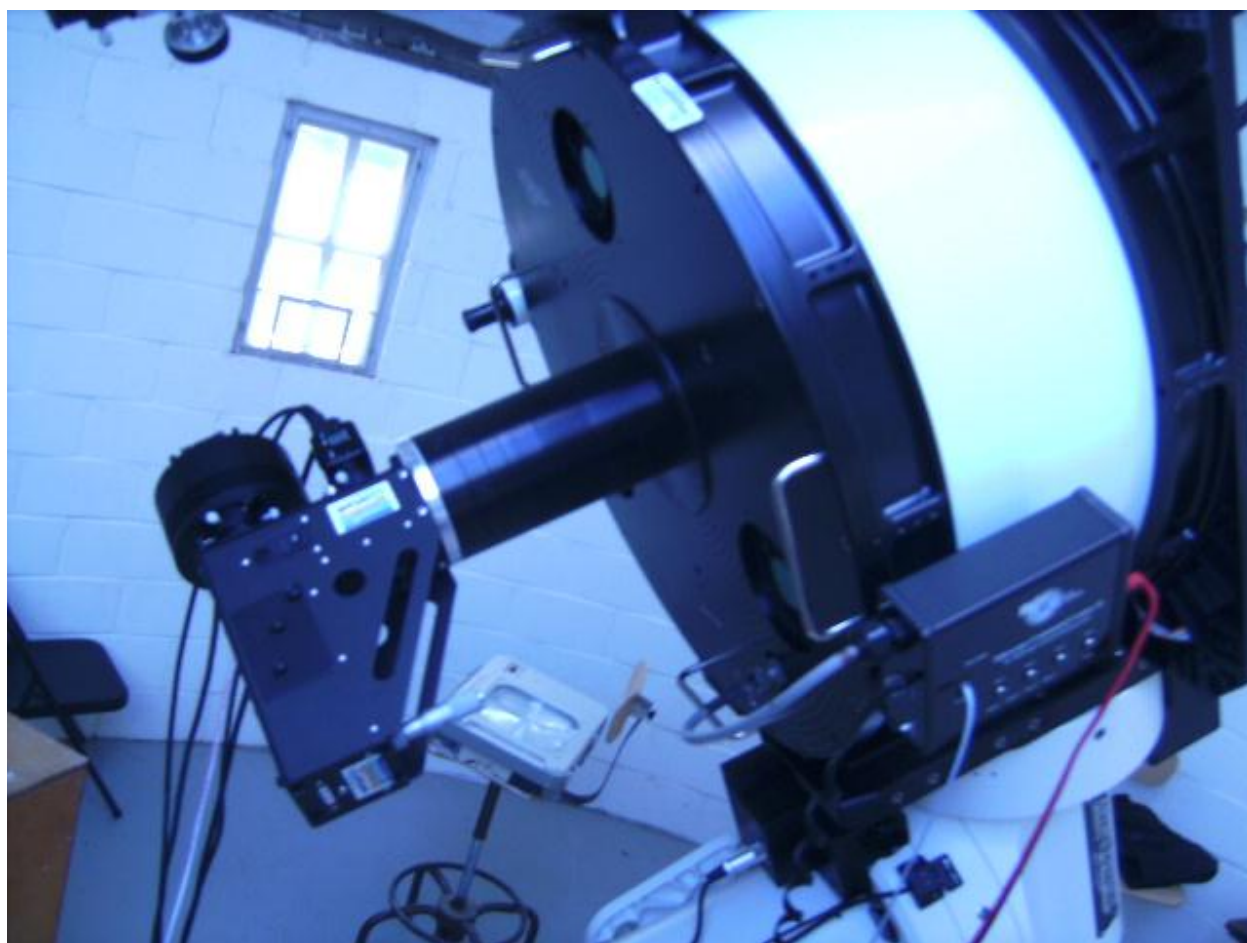


Figure 2.2: A view of the HLCO 20 inch telescope and spectrograph.

2.2.1 The Slit

There are currently two sets of slits which can be used with the spectrograph. One set is a series of four slits with settings of 15 μm , 19 μm , 23 μm , and 35 μm in width. The second set has the four settings of 19 μm , 50 μm , 75 μm , and 100 μm . The 19 μm slit in the second set has a “hole” in the center of the slit, effectively making a double slit. This might prove to have useful applications, but as of yet no work has been done with the second slit configuration.

These slits are all located within a framework which allows the slit plate to be rotated. The slit holder can be removed, the face plate disassembled, and the polished mirror turned to give a different slit width. It can thus be changed quickly mechanically. Figure 2.3 shows one slit. There is a second of these holders that houses the wider slits. It is easy to observe which slit is the one in the light path by simply turning the slit holder around and checking to see which of the slits is positioned over the hole that allows light through. There are numbers located in the corners of the mirror slit plate and these give the slit width in micrometers (μm). The given slit lies under the number to which it relates.

The choice of slit depends on the goals of the program. For example, studies of the spectral energy distribution require a good estimate of the total flux from the object, so a larger slit would be used. On the other hand, for radial velocity measurements or line profile studies higher spectral resolution is needed, so a smaller slit is generally preferred. (The one caveat is that you want a resolution no smaller than two pixels, in the case of our CCD, a slit size no less than 18 μm .) For fainter stars, a compromise must be made between flux (larger slit) and resolution (smaller slit). It will be left to the observer to determine the best fit for their intended target.



Figure 2.3: The highly polished slit plate. The numbers in the corners of the mirror correspond to the slit which is under the label.

These slits also are easily interchanged in the spectrograph. The access panel is on the bottom of the spectrograph, see Figure 2.4. Two thumbscrews hold it in place. By unscrewing these, the slit can be carefully eased free and changed, either by replacing the assembly with the second set, or by changing the slit by rotating the slit plate. The 23 μm slit width setting has been used for all data collection thus far.

The next thing to find is the angular size upon the sky that is associated with each slit. This is derived from the focal length of the telescope to determine the plate scale, and then the slit size can be found. Equation 2.1 is the equation for finding the plate scale,

$$P = f * \sin \theta \quad \text{Equation 2.1}$$

where P is the plate scale, f is the telescope's focal length, and θ is the angle on the sky. For the case of small angles $\sin \theta = \theta$, where θ is measured in radians, so the above becomes

$$P = f * \theta$$

and one can then solve for the scale. The telescope has a 20 inch or 0.508 meter aperture. The focal ratio is f/8.1. This gives a focal length of 4.115 meters, or $4.115 \times 10^6 \mu\text{m}$. Setting $\theta=1$ arcsec= $1/206265$ radians, one finds the result of $19.95 \mu\text{m}/\text{arcsec}$. Inverting this gives the number that we are interested in, $0.050 \text{ arcsec}/\mu\text{m}$. Multiplying this number by the slit size in micrometers gives the angular width and these are listed in Table 2.1.

Table 2.1: Angular Size of Slit upon the Sky.

Slit size (μm)	Angular size on sky (arcseconds)
15	0.75
19	0.95
23	1.15
35	1.75
50	2.50
75	3.75
100	5.00

2.2.2 Guide Camera

The guide camera currently in use is a WATEC IZON webcam, which was included in our purchase of the spectrograph, its field of view is about 10 arc minutes. It is run with a free, open source downloadable software program called VLC.⁵ This program allows us to stream the image from the guide camera and watch the star on the slit as we observe. Keeping the star on the slit is done manually with the computerized telescope controls (see Section 2.1 and Appendix A). As can be seen in Figure 2.1, the guide camera does not look directly at the slit but rather a mirror which reflects light back to the camera from the slit. There were some early minor changes needed so that the slit was centered in the middle of the mirror, however once set the mirror should need no further adjustment barring a disassembly of the spectrograph. Proper mounting procedure and guide camera startup can be found in Appendix A.2.3.

One modification to our camera is that there is a refresh rate and gain control paddle. This control box allows one to play with the guide camera signal to noise ratio to obtain dim objects, and keep bright objects to a manageable size on the guide camera CCD. There is a practical limit to how long one can allow the camera to accumulate counts before the star will drift from the slit. Anything longer than a ten second refresh rate is pushing this boundary. Both the gain and refresh rate will need to be adjusted depending upon the target being viewed. Dimmer object might be possible with new software that would subtract dark frames automatically.

⁵ Available from <http://www.VideoLAN.org>.



Figure 2.4: The Slit Access panel on the Spectrograph.

In our observing experience the guide camera is the limiting factor for the brightness of star which can be observed. Stars fainter than 6th magnitude become difficult to follow, and beyond 8th magnitude it is nearly impossible even with the gain and refresh rates pushed to the maximum limits. One of the hopes for our current spectrograph is to obtain spectra of galaxies and other faint objects. In order to do this, we will need to obtain both a better guide camera and some more advanced software to run our guide camera.

2.2.3 The Neon Comparison lamp

The spectrograph comes with a built in neon comparison lamp for wavelength calibration. A simple twist of a knob will place the comparison lamp in the optical path of the spectrograph. While a helpful tool for wavelength calibrations in the 5000 Å to 7000 Å range, the lack of intense blue lines make neon difficult to use for short wavelength observations. Another problem with the neon lamp is that there is a sufficiently large separation between lines that in some cases only two or three lines are recorded when using the 2400 g/mm grating. This can make one's wavelength calibration difficult. The tables of grating tilt and wavelength in Section 2.2.5 should be of some help here. One solution may be to use the Thorium-Argon (Th-Ar) comparison lamp that was used with the MTT spectrograph in the past. It has many more lines at the shorter wavelengths. Appendix A has more information concerning the use of the neon lamp while observing. As a general rule a comp lamp image should be taken anytime settings on the spectrograph are changed, and as often as the observer would like for calibration purposes of their target.

2.2.4 The Main Mirror and Collimator Focus

The positions of the main mirror and collimator are very important in obtaining the proper focus for the spectrograph. If these two components are not properly set then the data will suffer from a

variety of problems that can serve to make it unusable. The main mirror adjustment is simple. A screw is attached to the mirror bracket; one simply loosens the screw enough to allow it to slide up a slot. Figure 2.5 shows the position of this screw. It should be adjusted such that the image of the slit runs across the midpoint of the vertical axis of the CCD camera used for imaging. If this is not done and the angle of the mirror is too small, then there will be vignetting of the spectrum. If the angle is too large then the doublet lens may produce chromatic aberration.

The most important element of focusing is to set the collimator correctly. The collimator can be accessed by either of two access panels on the spectrograph. See Figure 2.6 for an image of one access panel. The large thumbscrew in the corner must be unscrewed and then the cover is slid back slightly and then pulled off the spectrograph. Removing this cover will expose the collimator, see Figure 2.7. To adjust this one simply uses a finger to twist the device, see Figure 2.8. A nylon set screw is present and that must be loosened to allow for motion. There is one on each side. It is not necessary to tighten these until the final focus is decided, as the collimator will not move readily. The focus will be complete once the neon comparison lamp lines are as fine and sharp as they can be made. Their full width half maximum (FWHM) should be somewhere around 3 to 4 pixels under the best circumstances according to the manufacturers for the 23 μm slit.



Figure 2.5: The Main Mirror Adjustment Screw. This screw is in its own slot, and does not need to be loosened much, only enough to slide. The proper position of this mirror is determined by the position of the projected slit upon the CCD camera



Figure 2.6: The Collimation Access Panel. Only the large thumbscrew in the upper left corner needs to be unscrewed, both of the others are fixed. There is an identical panel on the other side of the spectrograph.

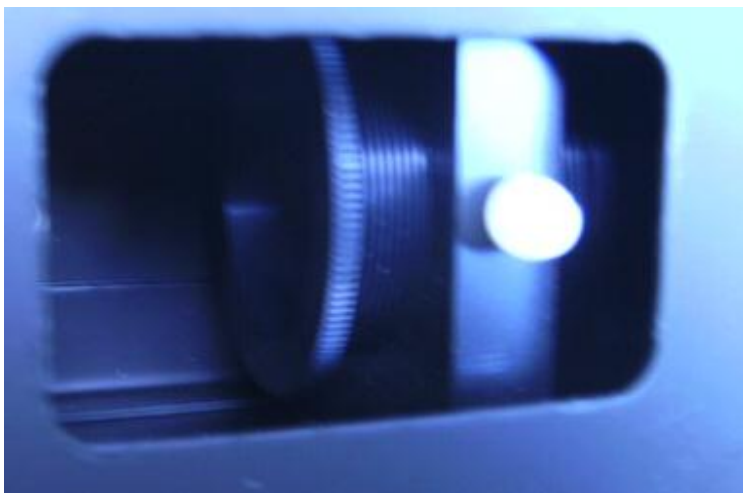


Figure 2.7: The Collimator. The nylon set screw can be seen as the white object in the right of the image.



Figure 2.8: Adjusting the Collimator. The focus is adjusted by rotating the collimator with your finger. It will be properly adjusted when the neon comparison lines are as narrow as they can be made. When making comparison lamp images, the cover will need to be replaced to prevent stray light from ruining the image.

2.2.5 The Gratings

There are three gratings that we ordered with our spectrograph: 2400 grooves (g)/millimeter (mm), 600 g/mm, and 150 g/mm. It was anticipated that these three gratings would give us a large range of resolutions, as well as wavelength ranges, to work within. The 600 g/mm and the 150 g/mm gratings are labeled, but the 2400 g/mm is unlabeled.

The 150 g/mm and 600 g/mm are ruled gratings blazed at 5000 \AA , while the 2400 g/mm grating is a holographic grating optimized for the visible range. See Table 2.2 for details. The three graphs, Figures 2.9, 2.10, and 2.11 below show their efficiencies for polarized light as a function of wavelength. The most important curve is the average. The lines marked S and P are where the electric field vectors are perpendicular and parallel to the grating facets.

Table 2.2: The Gratings and their Respective Blaze Angles.

Grating	Blaze angle
150 g/mm	$2^{\circ} 8'$
600 g/mm	$8^{\circ} 37'$
2400 g/mm	Holographic grating optimized in the visible range

To remove a grating from the spectrograph, unscrew the four thumbscrews in the corners, holding the grating to the spectrograph, see Figure 2.12. Also unscrew the micrometer to at least the 21 mm marking, to relieve the tension on the grating and to remove the arm from the path of travel. After a new grating is inserted, the four thumbscrews must be replaced.

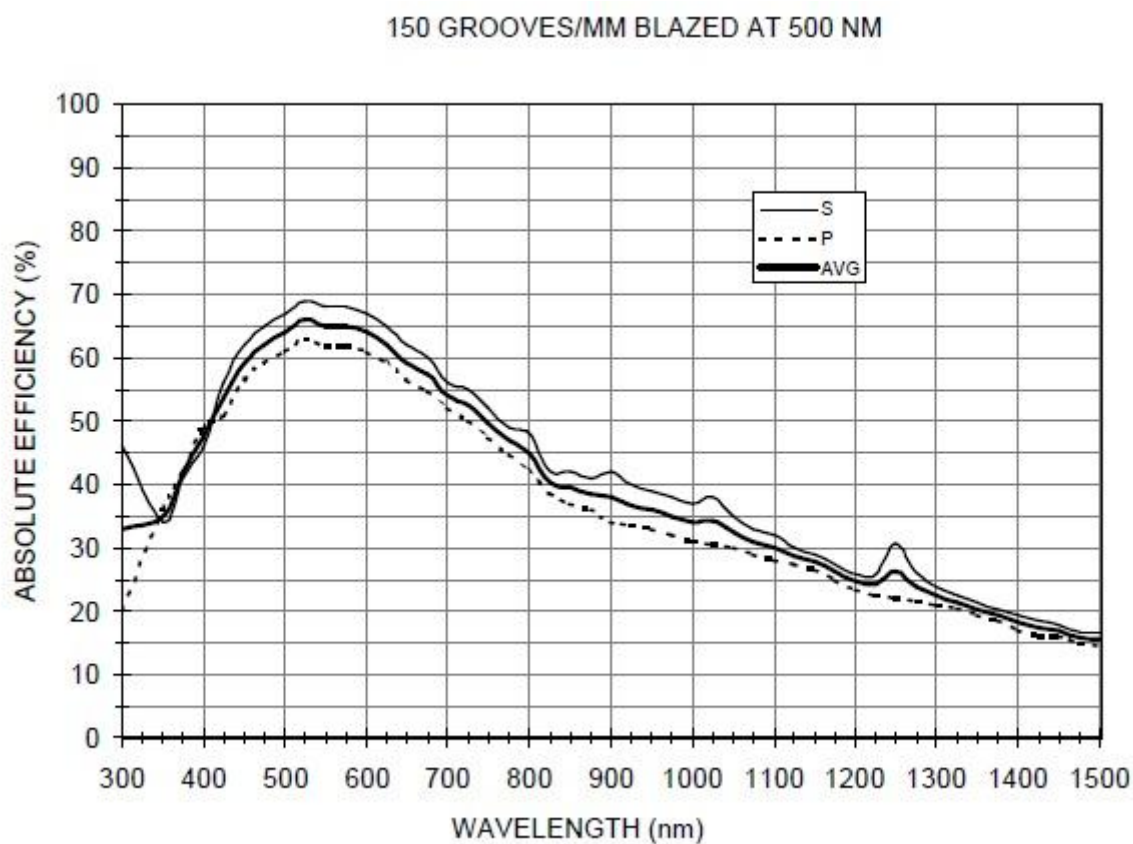


Figure 2.9: The blaze efficiency for the 150 g/mm grating. The line marked as S is perpendicular polarization, while the line marked P is for parallel polarization. The important line to look at is the average. Optimal efficiency occurs around 5200 Å. Image provided by Olivier Thizy (Shelyak Instruments).

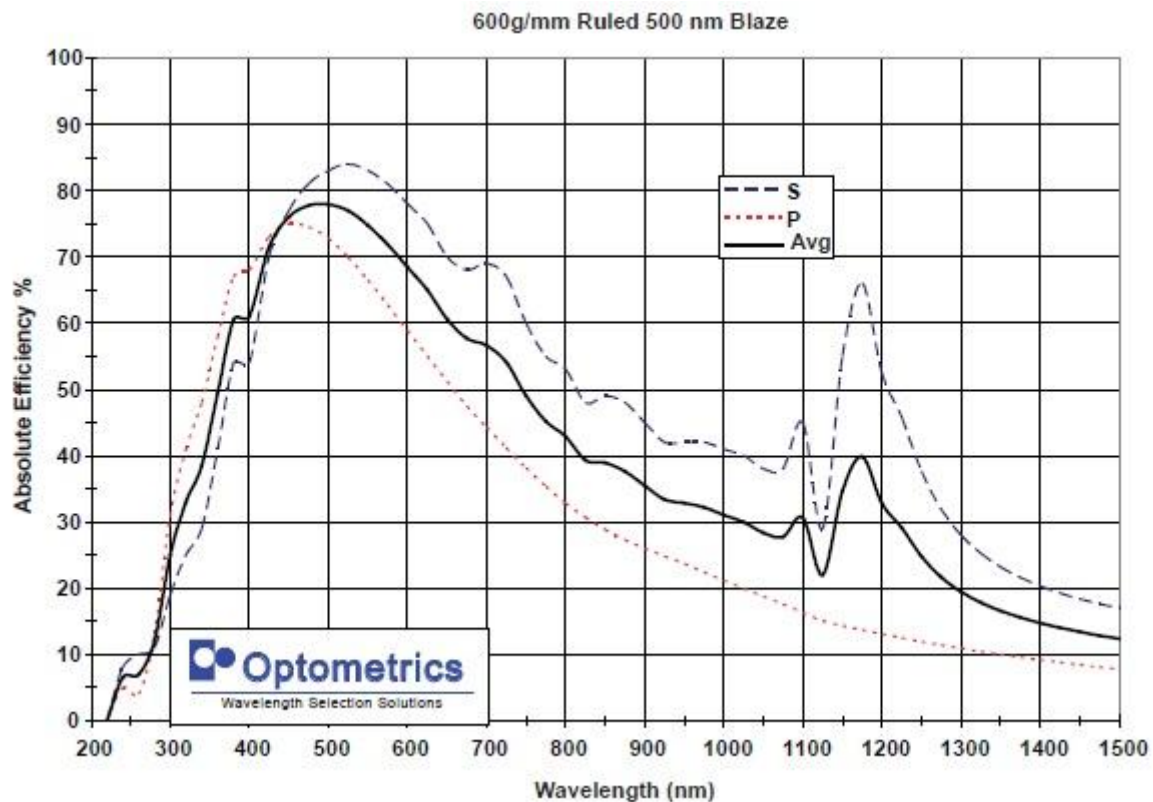


Figure 2.10: The blaze efficiency for the 600 g/mm grating. The line marked as S is for perpendicular polarization, while the line marked P is for parallel polarization. The important line to look at is the average. Optimal efficiency occurs around 4900 Å. *Image provided by Olivier Thizy (Shelyak Instruments).*

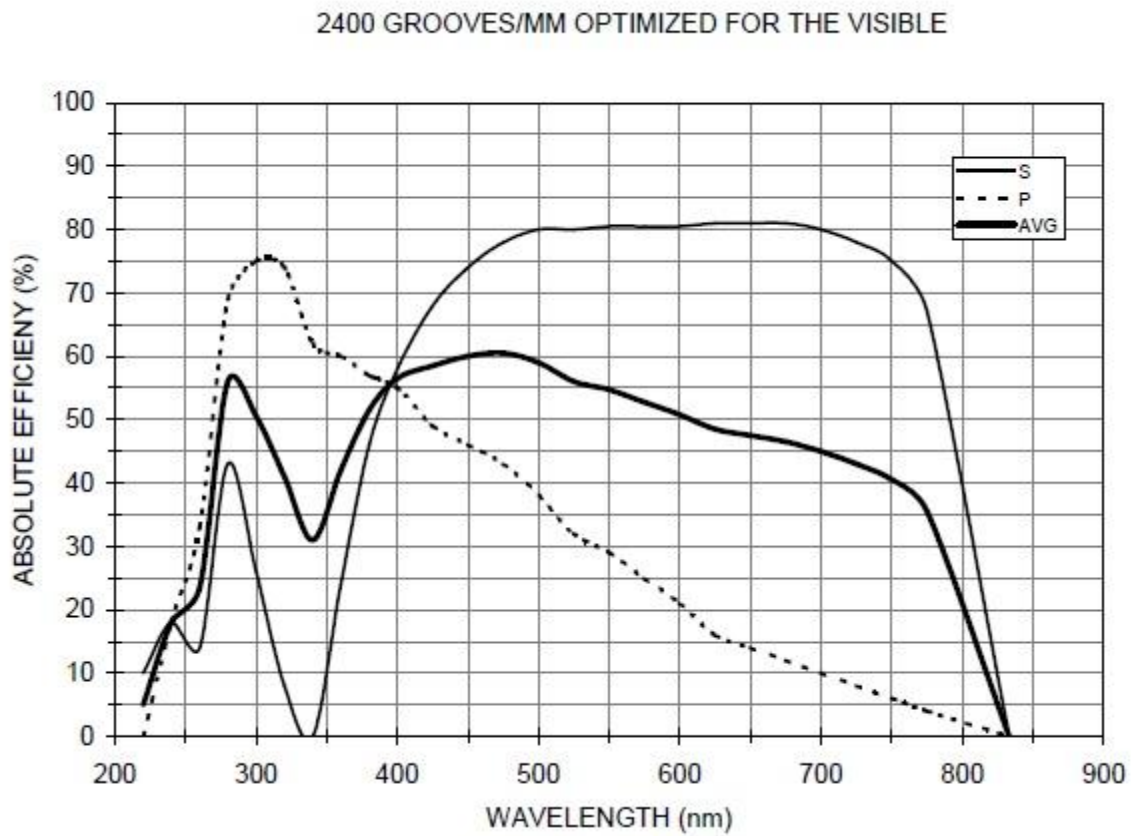


Figure 2.11: The efficiency for the 2400 g/mm grating. The line marked as S is for perpendicular polarization, while the line marked P is for parallel polarization. The important line to look at is the average. The best optimal efficiency is between 3000 Å and 7000 Å. *Image provided by Olivier Thizy (Shelyak Instruments).*

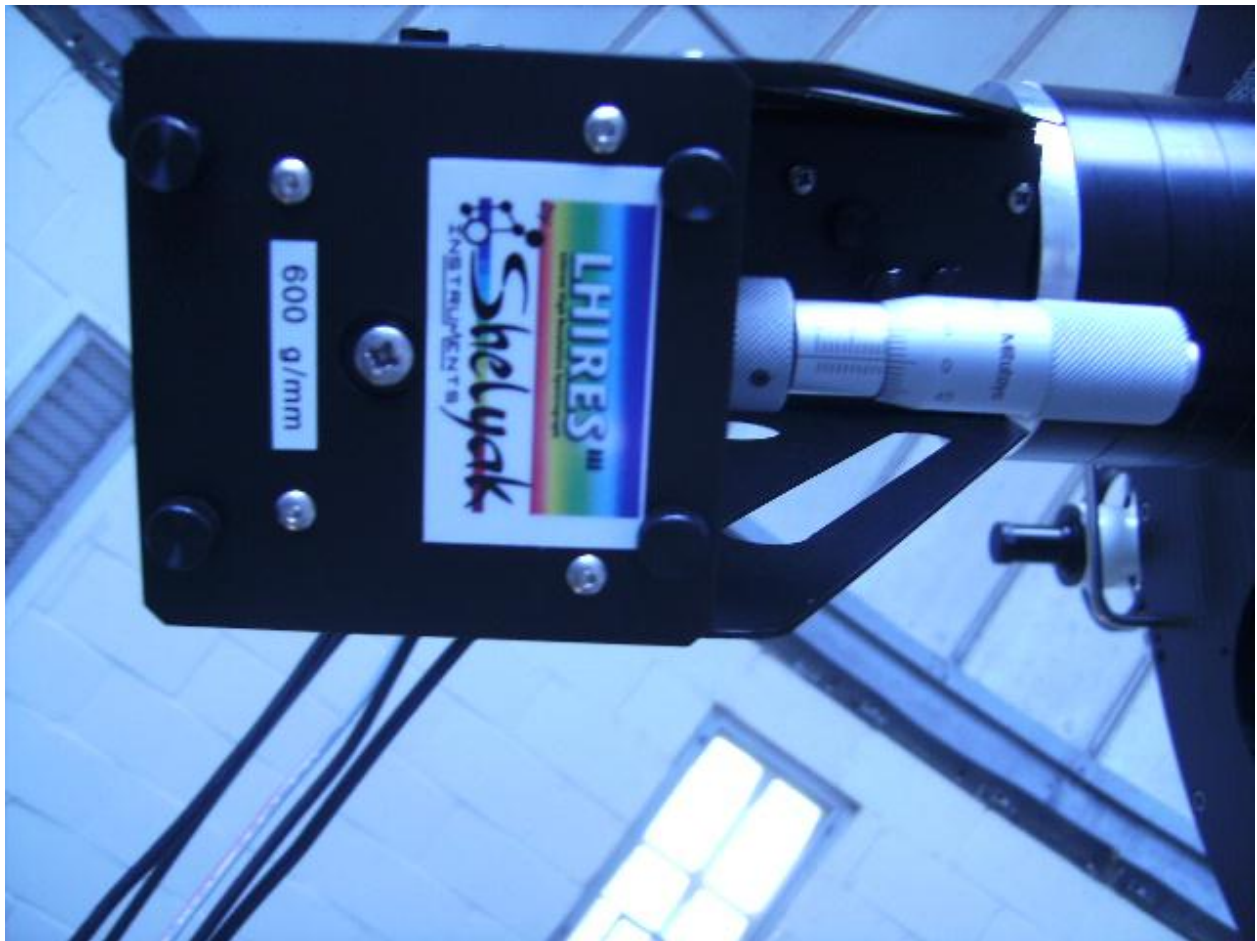


Figure 2.12: An image of the grating mount. The four thumbscrews are seen as the black knobs in the four corners. These need to be unscrewed and the micrometer needs to be dialed out past the 21 mm mark before removal is attempted.

Note that while the 2400 g/mm grating will barely fit the entire visible spectrum within the range of motion for the micrometer, the 150 g/mm will display secondary, tertiary, and higher order spectra within the range of motion. Even the 600 g/mm can display some of the second order spectra. The observer must be careful to be certain that the first order is being viewed at any particular time, the following tables will assist with this determination.

The grating tilt is set by a micrometer screw that pushes against a cylindrical bar that is set behind the grating in each grating mount, see Figure 2.13. Moving the micrometer screw outwards (to larger positional values on the micrometer) tilts the grating to a larger angle with respect to the light path from the collimator. This means a smaller the number on the micrometer shifts of the spectrum towards the blue. With the quasi-Littrow configuration of the spectrograph, the angle α of incoming beam to the grating normal equals the angle β of the outgoing beam to the grating normal. According to the grating equation (cf. Gray 2005), the central wavelength λ of the spectrum image at the detector is $\lambda = (2 d \sin(\beta))/n$ where d equals the grating facet spacing ($= 10^7 \text{ \AA/mm}$ divided by the number of g/mm) and n is the order of the spectrum (one at present).

We can determine the relation between the micrometer setting s and the grating angle β by examining the grating swivel geometry in Figure 2.13. The angle, β of the grating face to the optical axis equals the sum of two angles: γ = angle through the grating swivel point from the normal to the back of the grating to the center of the support cylinder, and δ = angle through the swivel point from the center of the support cylinder to the optical axis. Based upon Figure 2.13, $\gamma = 20^\circ$, and in what follows, let $c_1 = \sin \gamma$. The second angle, δ will be set by the micrometer screw length. Let s' equal the distance from the optical axis to the center of support cylinder, so that $s' = s + c_0$, where c_0 gives the zero-point offset of the micrometer. Then the angle δ is given

by $\sin\delta = s'/c_2$ where c_2 equals the distance from the swivel point to the center of the support cylinder (21.2 mm from Figure 2.13). Then the grating angle is $\sin\beta = \sin(\gamma + \delta) = c_1(1-x^2)^{0.5} + (1-c_1^2)^{0.5}x$ where $x = s'/c_2$.

The remaining unknown is c_0 , the zero-point offset of the micrometer screw. I found three micrometer settings that placed H-alpha (6563 Å) near the center of the spectrum: $s = (20.8, 10.5, 4.3)$ mm for the 2400 grating (first order) and the 600 and 150 gratings (second order), respectively. These correspond to $\sin\beta = (0.79, 0.39, 0.10)$, respectively, based upon the grating equation result above. The relation between micrometer position and $\sin\beta$ is shown in Figure 2.14 where these three measurements are plotted as diamonds. The solid line in the figure shows the relation given above for a best fit value of $c_0 = 9.48$ mm. Also shown as plus signs are the approximate measurements of micrometer setting and $\sin\beta$ (for central wavelengths obtained with the 2400 grating) from the LHIRES III User Guide.⁶ These are slightly offset from my results presumably due to a small difference in the micrometer zero-point value.

⁶ For more information see
<http://thizy.free.fr/shelyak/LhiresIII/DC0004A%20%20Lhires%20III%20User%20Guide%20-%20English.pdf>

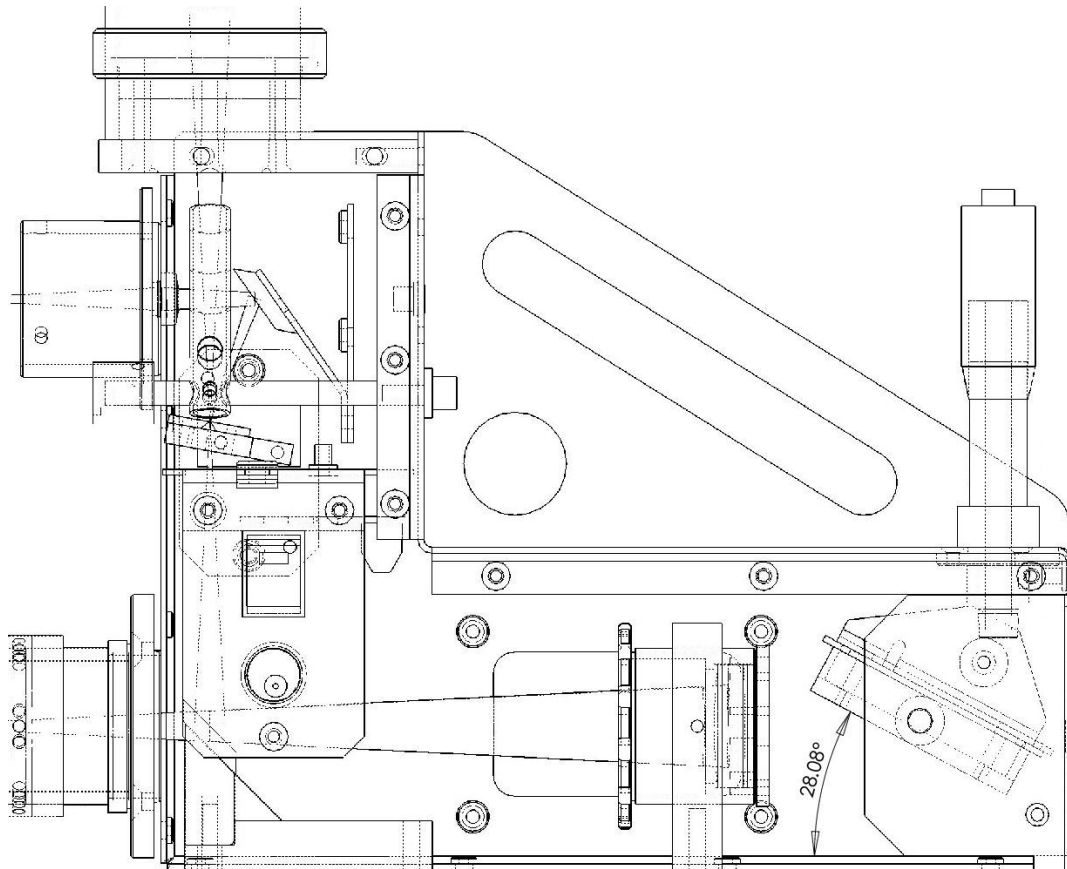


Figure 2.13: Mechanical Interior of the LHIRES III. Important to note is the micrometer motion and the two posts in the grating. The one not in contact with the micrometer is the swivel point. The other is the point at which the micrometer pushes the grating. *Image found at the manufacturer's website <http://www.astrosurf.com/thizy/lhires3/index-en.html>.*

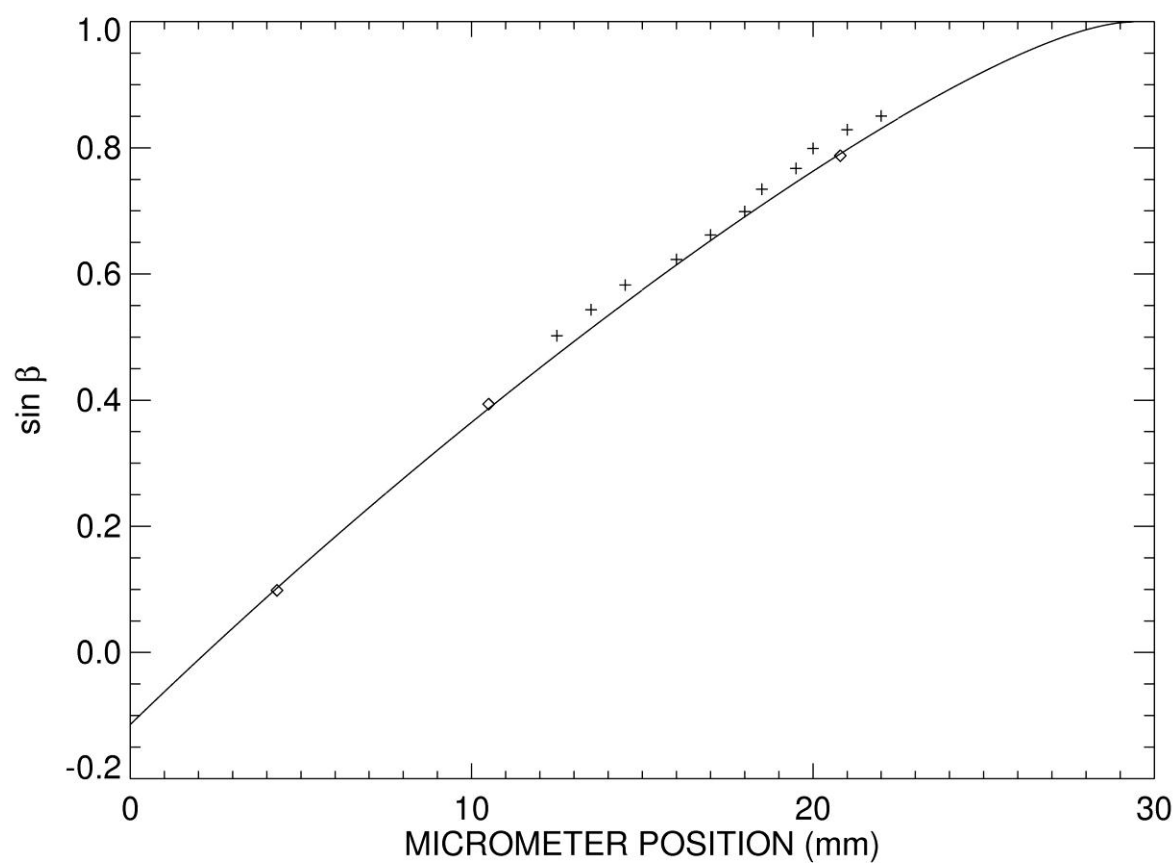


Figure 2.14: Micrometer position vs. $\sin \beta$. Using the points from our own observations (diamonds) a line is fit which shows the non-linearity of the motion. The crosses are points taken from the instruction manual for the LHIRES III as a comparison to our fit. The differences are likely due to minor construction differences.

Figure 2.15 shows the resulting predictions of the micrometer position and central wavelength for the three gratings (first order). These relations will need to be checked for hysteresis in the direction of screw motion. One simple way for observers to check that their tilt setting is correct is by observing the solar spectrum from the daytime sky and comparing to a solar atlas and/or by making Ne comparison lamp observations. Three tables are given below that list the micrometer settings as a function of central wavelength. These tables also list the spectral dispersion and wavelength coverage for use with the ST-8XE CCD camera. The spectral dispersion is given by Gray (2005): $d(\lambda)/d(x) = d \cos(\beta) / (n * f_{\text{cam}})$ where d equals the grating facet spacing, n is the order of the spectrum, and f_{cam} is the focal length of the camera/collimator lens (200 mm). This expression results in a dispersion measured in Å/mm, and in the tables below I multiply this by 0.009 mm/pixel to give units of Å/pixel. The spectral range is the dispersion multiplied by 1530, the number of pixels in the dispersion direction. The final column lists the spectral resolving power $R = \lambda/\Delta(\lambda)$. For a Littrow configuration where the collimator and camera focal lengths are equal, the projected slit width at the detector (FWHM) equals the actual slit width. The spectra presented here were made with the 23 μm slit, so $\text{FWHM} = 23 / 9 = 2.56$ pixels, and the resolving power was calculated with this assumption.

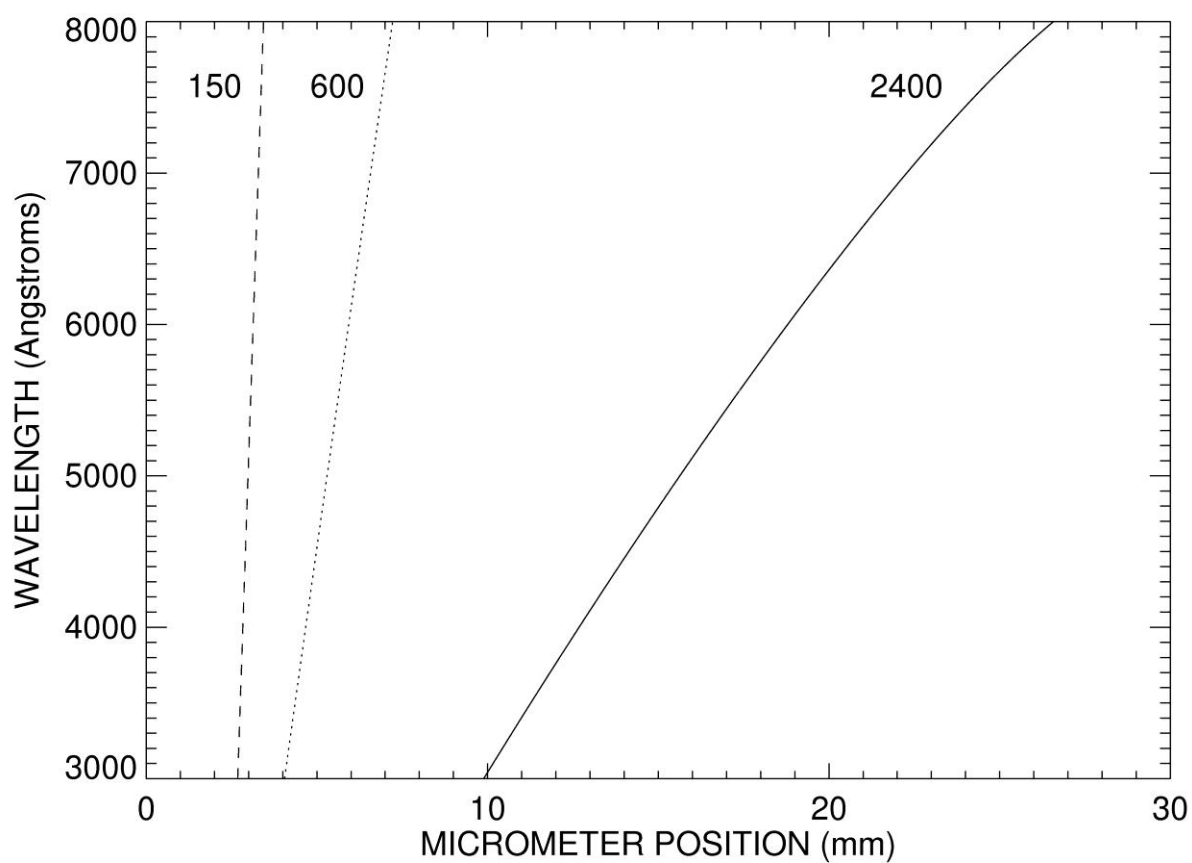


Figure 2.15: Micrometer position vs. Wavelength. This graph gives a general idea of the motion of the micrometer versus the wavelength of the first order spectra. It is of note that going to micrometer positions beyond these ranges will produce higher order spectra.

Table 2.3: 2400 g/mm Grating Data. The approximate micrometer setting which corresponds to a given wavelength, and the dispersion, spectral range, and the resolving power of that wavelength range.

λ (Å)	Micrometer Settings (mm)	Dispersion (Å/pix)	Range(Å)	R ($\lambda/\Delta\lambda$)
4000	12.68	0.164	251	9515
4100	12.97	0.163	249	9828
4200	13.26	0.162	247	10148
4300	13.55	0.161	245	10476
4400	13.84	0.159	243	10812
4500	14.14	0.158	241	11158
4600	14.43	0.156	239	11512
4700	14.73	0.155	236	11878
4800	15.03	0.153	234	12254
4900	15.33	0.152	232	12642
5000	15.63	0.150	229	13043
5100	15.94	0.148	226	13458
5200	16.25	0.147	224	13887
5300	16.56	0.145	221	14333
5400	16.87	0.143	218	14796
5500	17.18	0.141	215	15278
5600	17.50	0.139	212	15781
5700	17.82	0.137	209	16306
5800	18.14	0.135	205	16857
5900	18.46	0.132	202	17435
6000	18.79	0.130	199	18043
6100	19.12	0.128	195	18685
6200	19.46	0.125	191	19364
6300	19.79	0.123	187	20086
6400	20.14	0.120	183	20854
6500	20.48	0.117	179	21677
6600	20.83	0.114	175	22560
6700	21.19	0.111	170	23514
6800	21.54	0.108	165	24550
6900	21.91	0.105	160	25680
7000	22.28	0.102	155	26924

Table 2.4: 600 g/mm Grating Data. The approximate micrometer setting which corresponds to a given wavelength, and the dispersion, spectral range, and the resolving power of that wavelength range.

λ (Å)	Micrometer Settings (mm)	Dispersion (Å/pix)	Range(Å)	R ($\lambda/\Delta\lambda$)
4000	4.67	0.745	1139	2102
4100	4.74	0.744	1138	2155
4200	4.80	0.744	1138	2208
4300	4.86	0.744	1137	2262
4400	4.92	0.743	1137	2315
4500	4.99	0.743	1136	2369
4600	5.05	0.743	1136	2423
4700	5.11	0.743	1136	2476
4800	5.17	0.742	1135	2530
4900	5.24	0.742	1135	2584
5000	5.30	0.742	1134	2638
5100	5.36	0.741	1133	2692
5200	5.43	0.741	1133	2746
5300	5.49	0.740	1132	2800
5400	5.55	0.740	1132	2855
5500	5.62	0.740	1131	2909
5600	5.68	0.739	1131	2963
5700	5.74	0.739	1130	3018
5800	5.81	0.739	1129	3072
5900	5.87	0.738	1129	3127
6000	5.93	0.738	1128	3182
6100	6.00	0.737	1128	3237
6200	6.06	0.737	1127	3292
6300	6.13	0.736	1126	3347
6400	6.19	0.736	1126	3402
6500	6.25	0.736	1125	3457
6600	6.32	0.735	1124	3513
6700	6.38	0.735	1124	3568
6800	6.45	0.734	1123	3624
6900	6.51	0.734	1122	3679
7000	6.57	0.733	1121	3735

Table 2.5: 150 g/mm Grating Data. The approximate micrometer setting which corresponds to a given wavelength, and the dispersion, spectral range, and the resolving power of that wavelength range.

λ (Å)	Micrometer Settings (mm)	Dispersion (Å/pix)	Range(Å)	R ($\lambda/\Delta\lambda$)
4000	2.83	2.999	4587	521
4100	2.85	2.999	4587	535
4200	2.86	2.999	4587	548
4300	2.88	2.998	4587	561
4400	2.89	2.998	4587	574
4500	2.91	2.998	4587	587
4600	2.92	2.998	4587	600
4700	2.94	2.998	4587	613
4800	2.95	2.998	4587	626
4900	2.97	2.998	4586	639
5000	2.98	2.998	4586	652
5100	3.00	2.998	4586	665
5200	3.01	2.998	4586	678
5300	3.03	2.998	4586	691
5400	3.04	2.998	4586	704
5500	3.06	2.997	4586	718
5600	3.07	2.997	4585	731
5700	3.09	2.997	4585	744
5800	3.10	2.997	4585	757
5900	3.12	2.997	4585	770
6000	3.13	2.997	4585	783
6100	3.15	2.997	4585	796
6200	3.16	2.997	4585	809
6300	3.18	2.997	4584	822
6400	3.19	2.997	4584	835
6500	3.21	2.996	4584	848
6600	3.22	2.996	4584	861
6700	3.24	2.996	4584	875
6800	3.26	2.996	4584	888
6900	3.27	2.996	4583	901
7000	3.29	2.996	4583	914

The grating equation above shows that for any given angle β , there may be flux from other orders overlapping with the order of interest. As an example, a first order spectrum centered at 6000 Å may also record second order flux at 3000 Å, third order at 2000 Å, etc. In this case, there is no practical problem, since Earth's atmosphere effectively blocks all such low wavelength, ultraviolet flux from stars. However, above 3200 Å the atmosphere does begin to transmit stellar flux, and how much of such second order flux appears in a first order spectrum will depend on the wavelength dependent stellar spectral energy distribution, atmospheric transmission, glass transmission (through the collimator/camera lens), grating efficiency (see earlier figures), and CCD quantum efficiency (see Figure 2.17). Second order flux may become a significant problem for first order observations of hot stars in the wavelength range above 8000 Å. No observations should be attempted at present for orders greater than one since flux contamination from higher orders will be severe. For example, a second order spectrum of H-alpha at 6563 Å will also record first order flux at 1.3 microns (where the CCD is unresponsive) and third order flux at 4376 Å, and the overlap of the third order flux will significantly change the appearance of the spectrum. See Figure 2.16 for an example of this with the 600 g/mm grating. These problems can be solved by the introduction of order sorting filters into the light path, and it will be important to find a way to do this in the near future.

NOAO/IRAF V2.12.2a-EXPORT jenkins@swihart.chara.gsu.edu Wed 11:45:03 25-May
 [etaleo13.norm.f.fits]: 240. ap:1 beam:1

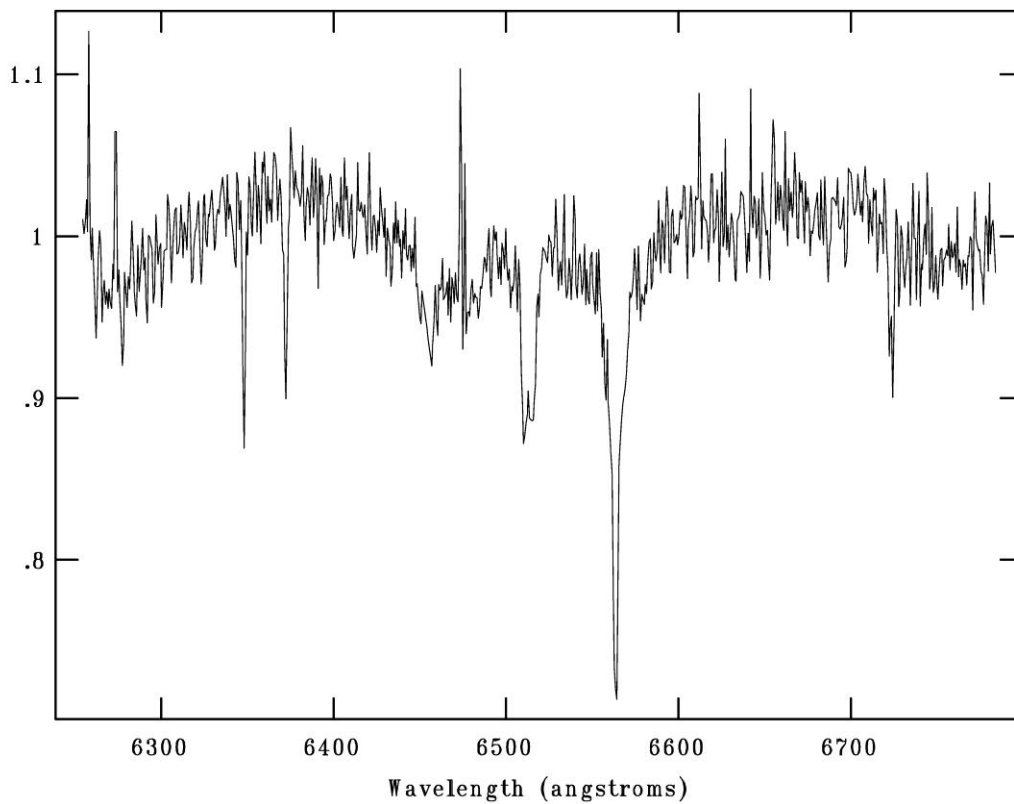


Figure 2.16: Example of Order Blending. This spectrum was taken with the 600 g/mm grating. It is a 240 second exposure near $H\alpha$, taken of η Leo on the night of UT 2011 May 7. The y-axis is a continuum normalized count. The second absorption feature, to the left of the $H\alpha$ feature is a third order $H\gamma$ feature which has been superimposed onto the second order spectral lines.

2.3 The CCD

The CCD which we are currently using with the spectrograph is the SBIG ST-8XME. This camera was originally used for imaging with the 16 inch Meade telescope, which the 20 inch replaced. It had an adaptive optics plate on it which was removed and replaced with a front plate from a SBIG ST-7 camera. The ST-7 was no longer in use due to problems with the coolers and slow communication with the parallel port connection. The ST-8XME has a resolution of 1530 x 1020 pixels, and each pixel is $9\text{ }\mu\text{m}^2$.⁷ The manufacturer lists the gain as 2.5 electrons and the read noise as 15 electrons. A graph of the quantum efficiency can be seen in Figure 2.17. Linearity tests were performed, and it was found that the camera loses its linearity after approximately 40,000 counts. See Figure 2.18 for our results. It is best to use a 1x1 binning scheme unless one is using a wide slit.

One of the issues with the ST-8 is that it has numerous hot pixels distributed randomly about the chip (see Figure 2.19). Not all of the white spots viewed are hot pixels, the large groupings of bright pixels are cosmic ray hits. These large spots were never observed to be in the same place between images. However the single bright pixels remain over many frames, and are present even with dark and bias frames removed. These are the hot pixels. Cooling to a temperature of lower than the -5°C , at which all of our observations were done, would help some with this issue, though this will only be an option in the cooler winter months with the ST-8XME. See Section 3 for an IRAF command to remove hot pixels from a spectrum. There has also been a suggestion of obtaining a new camera dedicated to the spectrograph as the ST-8 might once more be repurposed for the next project at HLCO, as an imaging camera for the 16 inch Meade in a new building.

⁷ More information on the ST-8 can be found at <http://www.sbig.com/sbwhtmls/ST8XME.htm>

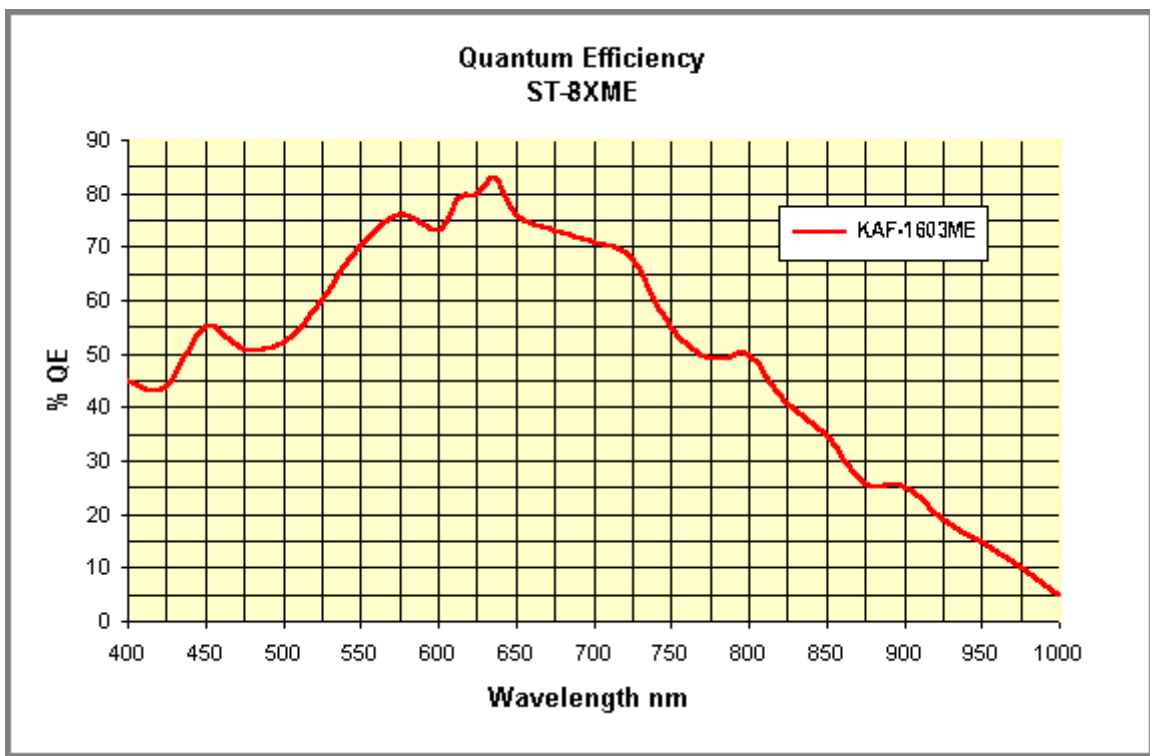


Figure 2.17: Quantum Efficiency of the ST-8XME. This graph shows optimal efficiency around 6350 Å at approximately 82%. Image found at SBIG website <http://www.sbig.com/sbwhtmls/ST8XME.htm>

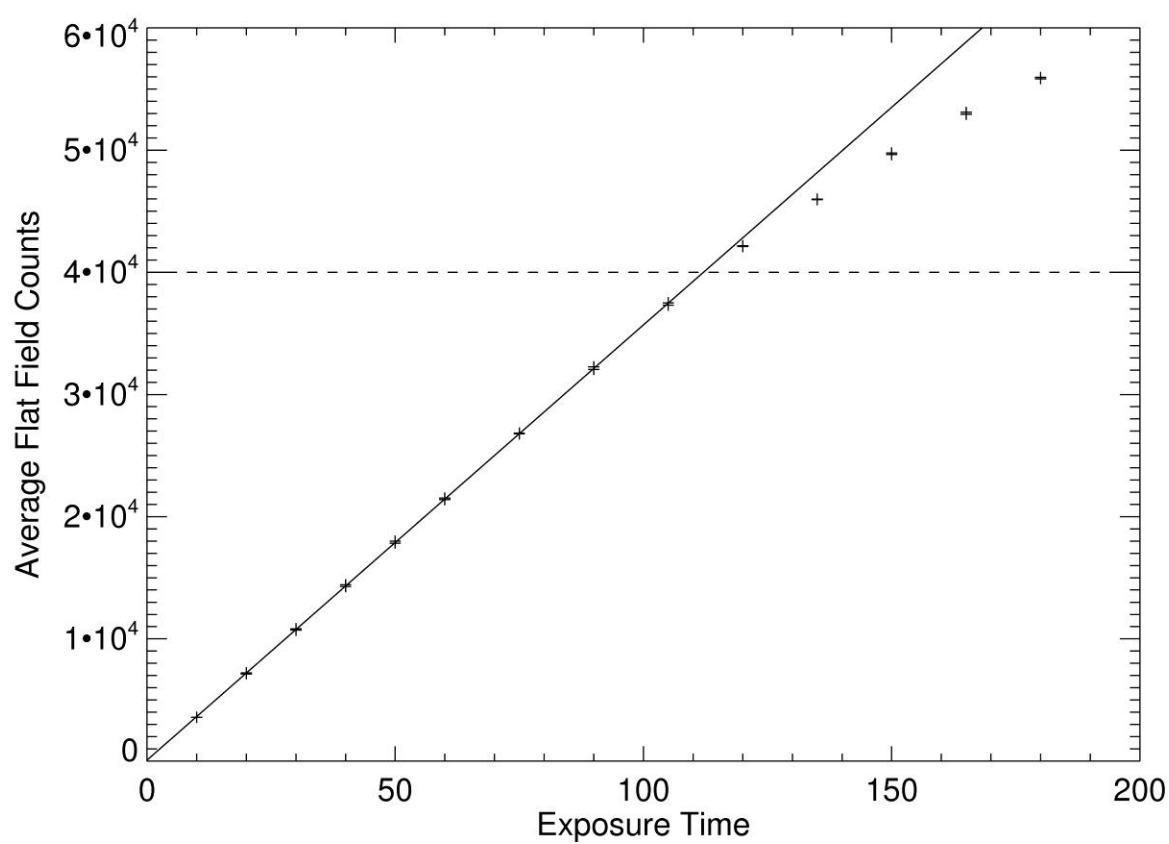


Figure 2.18: Linearity of the ST-8. Exposure time is in seconds. The light source used was an overhead projector halogen lamp. As can be seen the CCD loses its linear response around 40,000 counts.



Figure 2.19: ST-8 Hot Pixels. This is a dark and bias corrected image of Regulus taken May 7, 2011 with the 150 g/mm grating for 300 seconds. These are the high order spectral lines, hence the low signal to noise of the spectra, which can be seen running somewhat diagonally across the image. It shows the number of cosmic ray hits (multi-pixel groupings) and hot pixels (single pixels) spread across the image quite well.

3. REDUCING THE DATA

IRAF was used to reduce the data.⁸ Here I outline the basic methods used and how each result was obtained. The data were transported from HLCO via data stick and uploaded onto a machine with IRAF. These files were stored in a folder labeled with the year, month, and date of the observation to facilitate quick identification. Names of the flats, bias, and dark frames all began with the name of the respective type of frame. This made it easy to identify these files once looking at a list in IRAF.

Upon opening IRAF, the **noao**, **imred**, and **ccdred** packages are compiled. A header change must be done as the fits header reads out the bias files as a bias, and IRAF needs the header to read in as a zero. Once the header is changed, the bias frames are combined using the **zerocombine** function. The bias frames are removing differences in the initial pixel sensitivity from the image. The combined bias frames are then applied to all images using **ccdproc**. This process is repeated for the darks. The header for the dark frames must be changed so that the image is a dark. The **darkcombine** command is used to stack the darks, and then **ccdproc** is used, noting that a dark correction is being applied. This process is removing hot pixels from the image. Lists of the flat frames which correspond to a set of images should be created and then these flats are stacked together with the **flatcombine** command. This is removing the differences in pixel sensitivity during the imaging from the image. These combined flats should then be applied using **ccdproc** to only the corresponding image set, making certain that a flat correction is being applied and that the proper flats are being used.

⁸ IRAF is distributed by the National Optical Astronomy Observatory, which is operated by the Association of Universities for Research in Astronomy (AURA) under cooperative agreement with the National Science Foundation

Once all of the images have been corrected for the bias, dark, and flat frames, the spectra must be extracted from the image. To do this the **kpnoslit** package is loaded. Once the package is loaded the command **apall** is used to find the aperture size for the spatial dimension of the spectrum. This will need to be done for all the object images, though not for any comparison lamp exposures. After the aperture is located and the output spectrum has been extracted and saved, the **apsum** command is used to extract the comparison lamp spectrum and perform a wavelength calibration. The **identify** command is used to identify the lines visible from the comparison lamp spectra. For this step a general knowledge of the wavelength range being viewed is helpful, and an atlas of the neon lines is needed.

Once the information is written for the wavelength range, a header change must be done to associate a given object spectrum with the comparison reference spectrum. Then the **dispcor** command is entered to establish the wavelength calibration and to apply it to set the dispersion relation of the object spectra. To view the spectra **splot** was used. The **continuum** command was used to normalize the spectra. A known issue with the ST-8XME is a random smattering of hot pixels spread out over the chip (see Section 2.2.5). They are nearly impossible to avoid, but they can be subtracted out by going to the pixel position in **splot** and pressing the z key with the pointer on each side of the feature, thus replacing the hot pixel with a linear interpolation. This was done with a number of spectra.

Changes to this procedure must be adopted when there are no neon comparison lines in the wavelength range of interest, as when observing in the blue end of the spectrum. The wavelength calibration can be found instead by observing a well-known, late-type giant star. This was the case for our observations of α Vir in the 4520 Å waveband. In this instance a spectrum was taken of a star with a solar type spectrum and known radial velocity. For our observations ϵ Vir was

used. It is a magnitude 2.85 star with a spectral classification of G9 III. This spectrum was compared to stellar models and the wavelength solution found was then applied as a wavelength calibration of the α Vir spectra. In Figure 3.1, we show an observed spectrum of ϵ Vir (bottom) with a model synthetic spectrum (above) from the grid of Rodriguez-Merino et al. (2005). The model is based on stellar parameters for ϵ Vir from Takeda et al. (2008). The model makes a good match of the observed spectrum and can be used to calibrate the wavelength scale.

Calibration was done by cross-correlating the spectrum in 30 wavelength bins where an approximate linear wavelength calibration was used to map the model into pixel space. This provided a relation between mean pixel number and mean wavelength for 30 bins, and then a parabolic fit was made for wavelength as a function of pixel number. Figure 3.2 shows the differences in wavelength between the linear model and observed position along with the quadratic fit of the trend. Unfortunately, this provides only an approximate wavelength calibration for target spectra because the spectrograph suffers some flexure in moving between the target and calibrator. It may be useful in the future to use the department's Th-Ar lamp from the MTT spectrograph calibration unit in such cases. The Th-Ar source has many more lines that can be used directly to obtain the wavelength calibration, this lamp is currently being reprocessed for this purpose.

Another important consideration is that the observer must change from an earth based velocity to a heliocentric velocity. This can be done in IRAF via the following procedure. First run all spectra through **rvcorrect** to get VHELIO keyword in header. This requires one to load the following packages **noao**, **astutil**, and use the task **rvcorrect**. Using the **observatory** command the information for the observatory was filled in including Latitude, Longitude, altitude, and time zones. For HLCO these correspond to longitude = 83.593°, latitude = 33.6597°,

altitude = 210 meters, and time zone = 5. Using the **hedit** update the header with the object name, RA, DEC, and epoch data, if not already done at the telescope. Then use **asthedit** with file cmd: `st = mst (@'date-obs', obsdb ("obsvars", "longitude"))` to add the Sidereal time to header. Run **setjd**, then run **setairmass**. Check **keywpars** for name correspondence. Finally run **rvcorrect**.

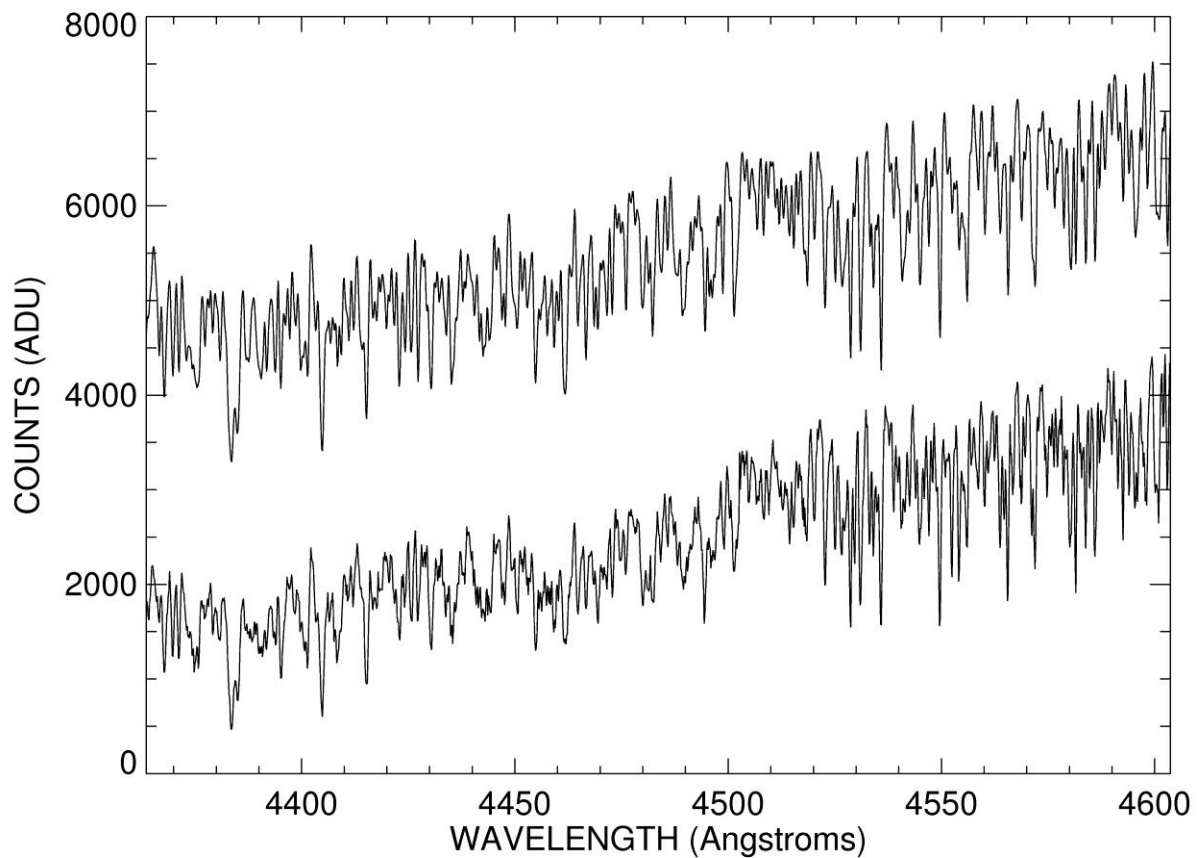


Figure 3.1: Wavelength Calibration. The observed spectrum of ϵ Vir (bottom) is compared here to a model synthetic spectrum (above) from the grid of Rodriguez-Merino et al. (2005). The model is based on stellar parameters for ϵ Vir from Takeda et al. (2008). With a good comparison, a wavelength calibration is made possible.

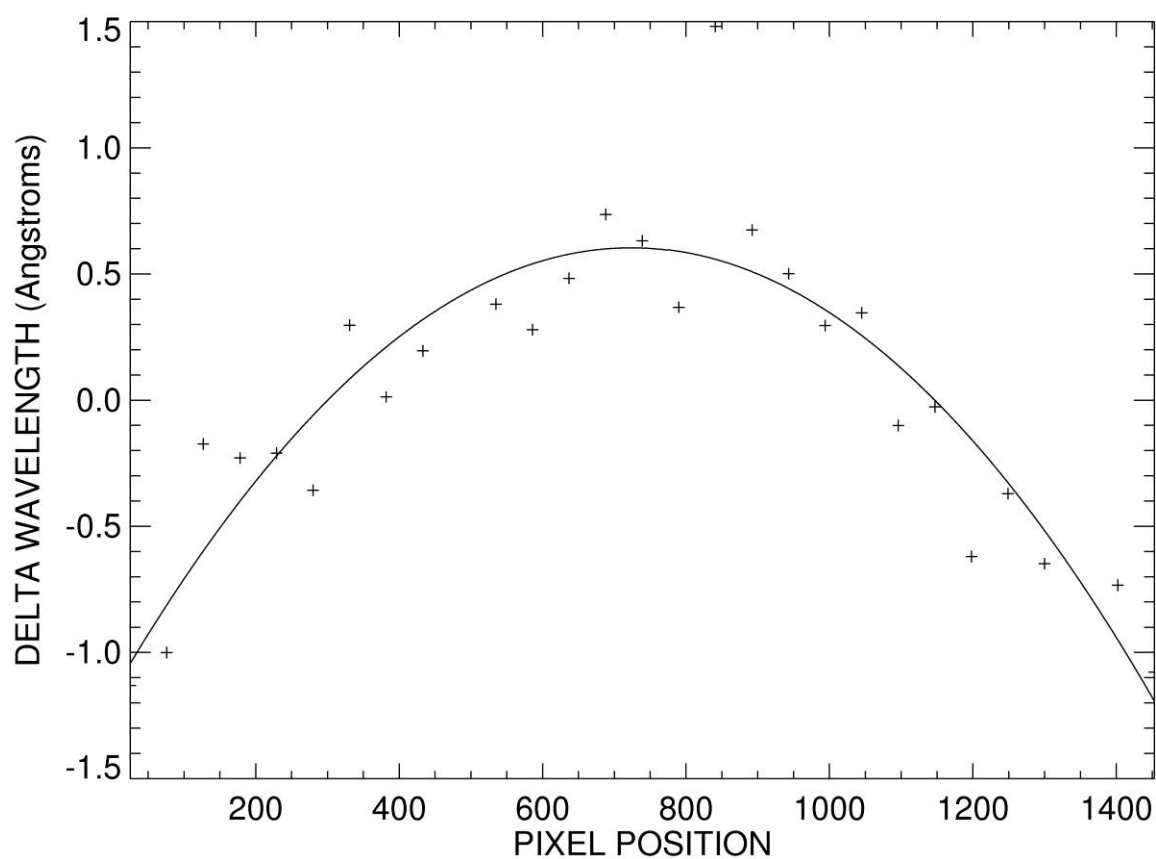


Figure 3.2: Calibration Variation. Here the differences in wavelength between the linear model and observed pixel position are shown. The line is the quadratic fit of the trend.

4. RESULTS

Once all the data had been reduced and wavelength calibrated, then science analysis may begin. Since targets with strong H α (6563 Å) lines were picked initially, we made sure to include that feature in the wavelength range. This was also important because much of the early work with the spectrograph involves observations of hot “Be” stars. The primary feature of interest in these stars is the H α emission line, and so characterization of the spectrograph in and around the H α feature will give other researchers a head start on their own data.

All of the data concerning the grating tilts appears in Tables 2.3, 2.4, and 2.5. These give the dispersion range and resolving power for each grating. Also included are the data for how a change in the micrometer setting relates to a wavelength shift. Again note that range of motion is not a linear progression across large wavelength changes. The same is true of the spectral range. At bluer wavelengths the window of visible wavelengths is larger. At redder wavelengths, it is reduced in size. Appendix A is a compilation of notes and handy tricks which have been discovered to aid the observer with things learned from experience. Between the tables and Appendix A it is likely many of the issues facing the observer have been answered.

Another set of values of interest are the signal to noise ratio for the gratings of our spectrograph. A figure of merit for the 2400 g/mm can be found from our observations of α Vir. We had observations running for a length of five minutes for over five hours on the night of UT 2011 May 19. During these five minute observations of the 0.91 apparent magnitude star in B band with the 2400 g/mm grating, we were getting SNR of approximately 600/pixel in the range of 4578 Å to 4585 Å, within the continuum. The number of counts in the raw exposures was around 3700 ADU with the above parameters. This is in the blue end of the spectrum where the

QE of the CCD suffers, and yet it still places the SNR of our observations on par with measurements made of α Vir with the MTT (Riddle 2000).

Calculation of the SNR follows Poisson statistics, such that the SNR goes as the square root of the signal. Things which affect the SNR are the magnitude of the object being viewed, exposure time, resolving power, and the slit size. Also, to a lesser extent grating efficiency and the CCD efficiency. Here we will look at a quick example of transitioning to an 11th mag object with 600 g/mm grating. From our α Vir 0.91 mag with the 2400 g/mm grating. Since $\Delta m = -2.5 \log \frac{F_2}{F_1} \approx 10$. That gives that $0.0001 = \frac{F_2}{F_1}$. This mean that the $\frac{S}{N} = \left(\frac{S}{N}\right)' * \sqrt{S} = \frac{600}{\sqrt{10000}} = 6$. However, the 600 g/mm has a Resolving Power that is approximately 4 times reduced from the 2400 g/mm, such that $\frac{S}{N} = 6 * \sqrt{4} = 12$. Then assuming that one were to take a 1 hour exposure rather than the 5 minute exposure which we took for α Vir; $\frac{60}{5} = 12$ times longer, so that now $\frac{S}{N} = 12 * \sqrt{12} = 41.5$. Since one would like a SNR of 10/pixel or more the LHIRES III is likely able to obtain spectra with these parameters. However depending upon the wavelength viewed and the size of the slit opening there might be more gain then is listed here. Another issue which must be addressed is that at lower magnitudes the assumptions which govern the Poisson statistics breaks down as the noise from the dark current, sky, and read noise of the CCD become more prominent at the longer exposures.

Two sample spectra are shown. Figure 4.1 is a typical 2400 g/mm spectrum. It is a 90 second exposure of δ Sco which is a “Be” star. The double emission in the H α peak originates in flux from the circumstellar disk surrounding the star. The bluer peak is caused by the side of the disk which is rotating toward us, while the red peak is from the part of the disk receding.

Figure 4.2 is an interesting look at Deneb. Richardson et al. (2011) performed a five year high resolution spectroscopic and photometric survey on the prototypical alpha-Cygni variable supergiant, Deneb. In their analysis, they observed a "high velocity absorption event" in the fall of 2001 (HJD 2452150 -- 2452250) where a secondary absorption component appeared on the blue wing of the H-alpha profile, which shows a weak P Cygni type absorption and emission component from the modest wind. This secondary absorption disappeared at the end of this event, and this outflowing material seemed to then fall back towards the star, resulting in a redshifted absorption component. Our commissioning period spectra of Deneb shown in Figure 4.2, obtained with the 2400 g/mm grating, show a remarkable similarity to the data of Richardson et al. (2011). There is a secondary high-velocity (at -130 km/s) absorption component seen on UT 2011 May 10 that had vanished by the following observation on UT 2011 May 24. It would appear that we have caught Deneb in a state similar to that in 2001 when the high velocity absorption event occurred. Richardson et al. (2011) compared their results to that of other similar temperature supergiants, and found that Deneb is near the lower limit in temperature (~8500 K) for which these events can occur.

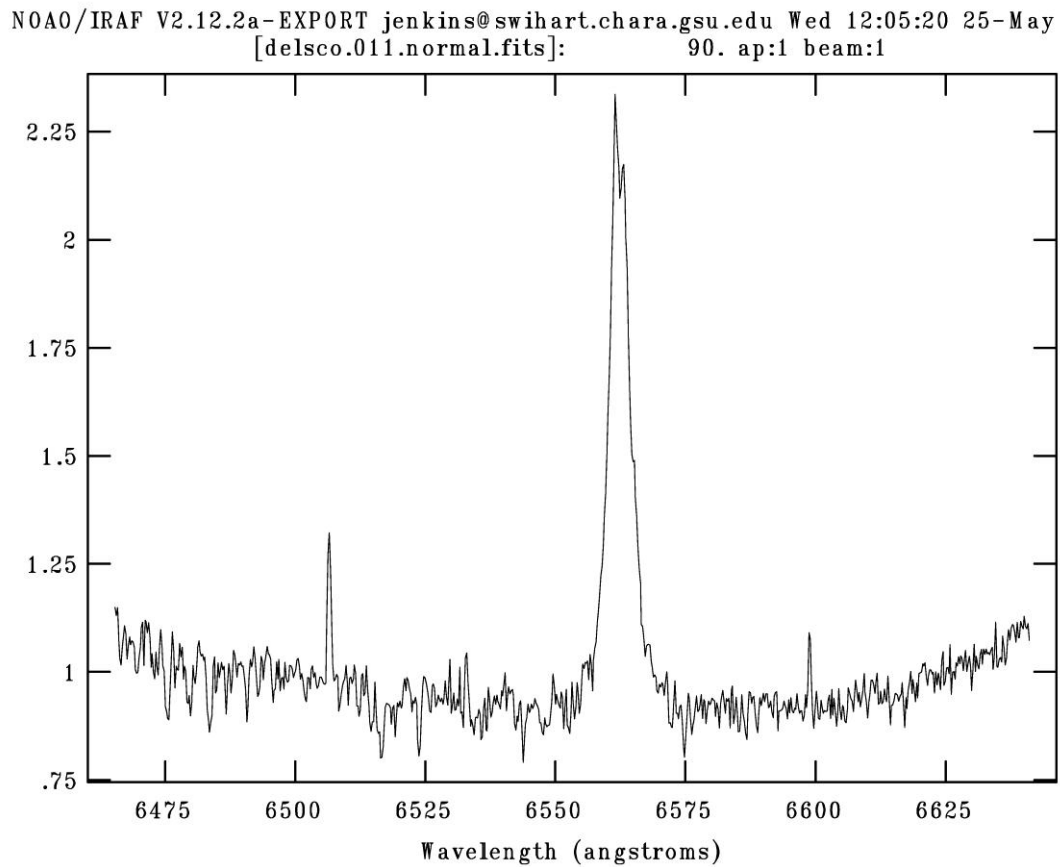


Figure 4.1: Sample Spectrum using the 2400 g/mm Grating. This is a 90 second exposure taken at H α of δ Sco. The strong H α feature can easily be seen. The y-axis is a continuum normalized count.

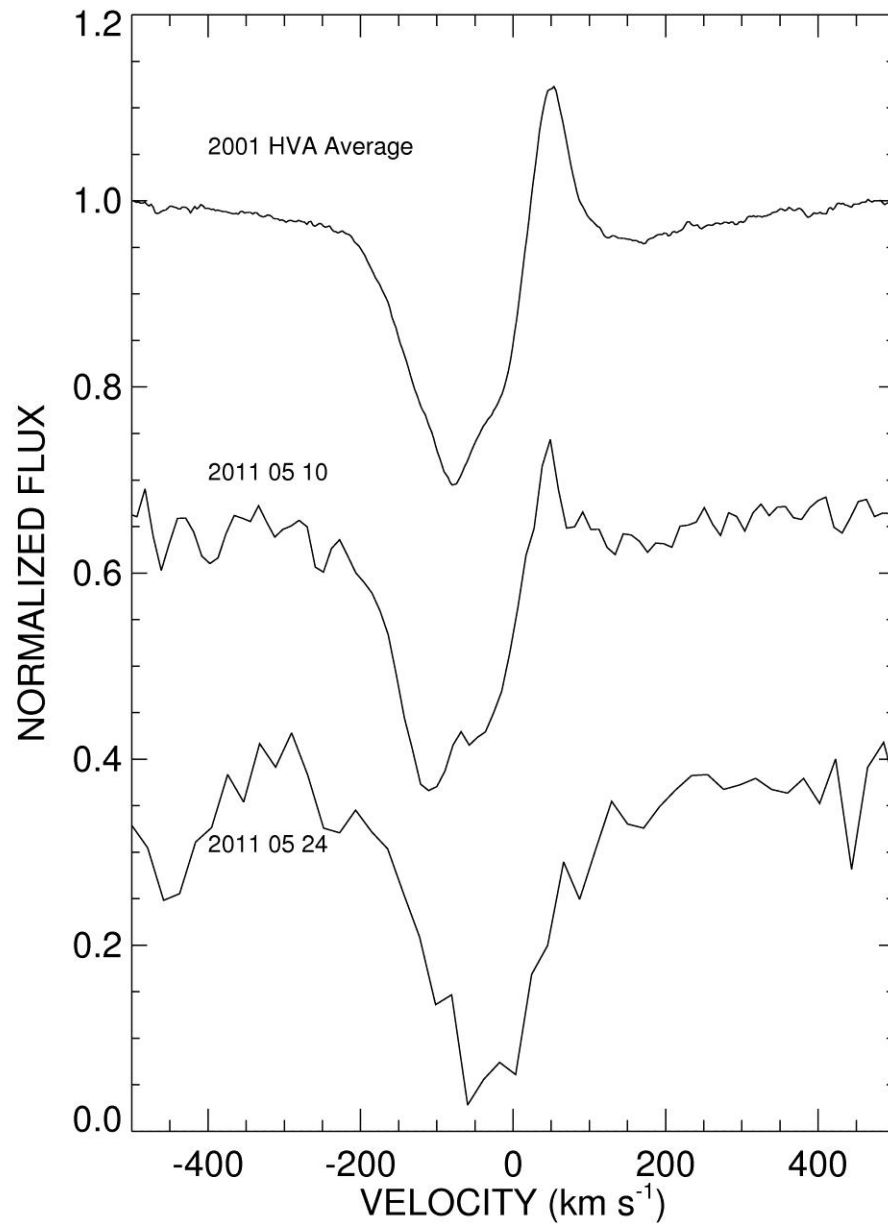


Figure 4.2: Spectra of Deneb. As can be seen in this figure the observations we have made of Deneb (middle and lower spectra) have features in the P Cygni profile which resemble a similar blue shifted absorption that was observed by Richardson et al. (2011).

5. OBSERVATIONS OF α Vir = HD 116658

In an effort to show the true potential of the newest research tool at our disposal, I decided to observe the star α Vir, known better by its common name of Spica. α Vir is one of the nearest massive binary star systems. It is a double-lined spectroscopic binary with an orbital period of 4.014 days (Riddle 2000).

Spica was observed on the night of UT 2011 May 19 using the 2400 g/mm grating in the 4520 Å waveband. Exposures were made for 300 seconds each with a total of 45 spectra for the night. No block of observations exceeded one hour before a comparison spectrum was taken of ϵ Vir in an effort to obtain reliable zero point estimate for radial velocity measurements. Data reduction was completed as described in Section 3. I made 90 second exposures of ϵ Vir that were used to make an approximate wavelength calibration as discussed previously in Section 3. All 45 spectra were then transformed to a standard $\log \lambda$ wavelength grid with an increment equivalent to a Doppler shift of 10 km/s.

The average spectrum is shown in Figure 5.1 (top) together with a model (below) from the grid of Lanz & Hubeny (2007). The stellar parameters for this model are taken from the work of Harrington et al. (2009). The strongest lines are those of He I 4387 and 4471 Å, and the observed and model spectra make a good match for a stellar effective temperature of 26500 K. Note, however, that Spica is a double-lined spectroscopic binary and no allowance was made for the flux of the fainter companion in making the comparison with the models. The fainter companion is predicted to be red-shifted at the time of my observations (Harrington et al. 2009), and the companions Si III 4552 line might be present as the weak feature seen immediately to the right of the main profile in Figure 5.1.

Figure 5.2 shows a close up of the spectral region surrounding the triplet Si III 4552, 4567, 4574 Å. The observations are shown in the lab frame in this depiction, and they are separated so that the continuum is aligned with the time of observation indicated on the y-axis. The breaks in the observations are when comparison spectra were taken of ϵ Vir. Due to the fact that for much of the night ϵ Vir was across the meridian from α Vir, the slewing took some time. There were clearly systematic profile variations present at the time of the observations that appear prominent in the line cores. Harrington et al. (2009) argue that these variations result from the varying tidal pull of the companion that excites surface waves on the primary star. These oscillations create small Doppler shifts that add or subtract from the rotationally broadened profiles to create the patterns of line variability. The Doppler shift in the profiles' can be seen in Figure 5.3, and it is seen that contrary to what is reported by Harrington et al. (2009) and Riddle (2000), our variability is moving from red to blue wavelengths. Table 5.1 has the associated data as well as the errors for the radial velocities. The HLCO observations of Spica demonstrate that the LHIRES III spectrograph is a very useful instrument to explore such variability in this and other stars.

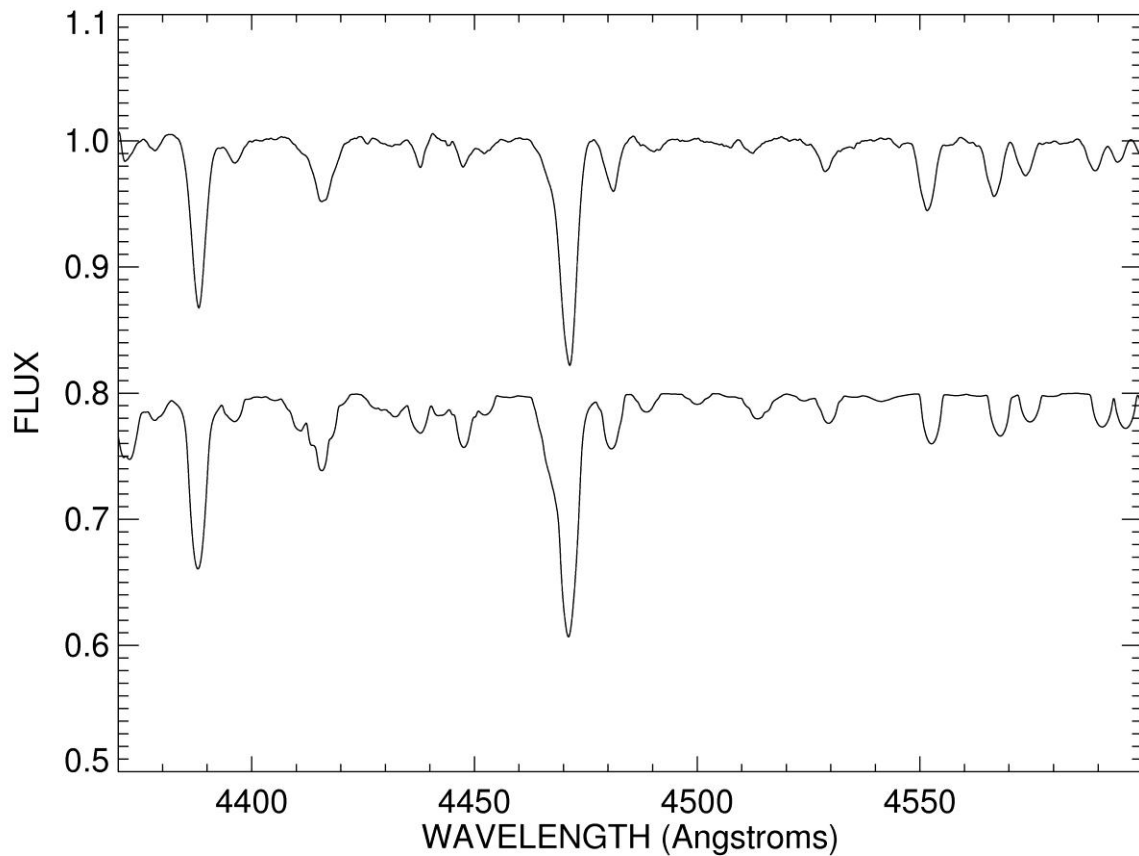


Figure 5.1: The average spectrum of α Vir (top) compared to the model (below) taken from the grid of Lanz & Hubeny (2007). The stellar parameters for this model are taken from the work of Harrington et al. (2009). The strongest lines are those of He I 4387 and 4471 Å. Note that Spica is a double-lined spectroscopic binary and no allowance was made for the flux of the fainter companion in making the comparison with the models.

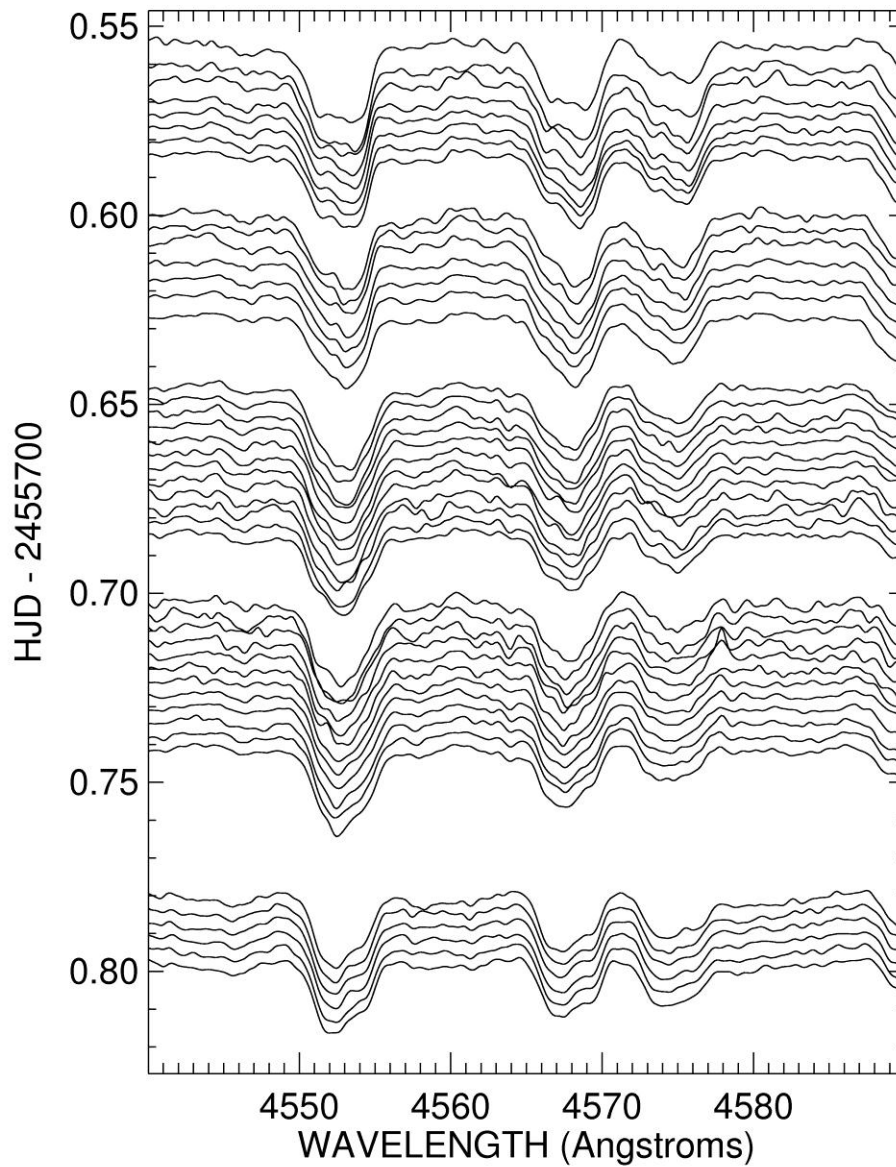


Figure 5.2: Line profile variability of α Vir. This is a close up of the spectral region surrounding the triplet Si III 4552, 4567, 4574 Å. The continuum is aligned with the time of observation on the y-axis. Breaks occur when comparison spectra were taken of ϵ Vir. A substructure in the profile can be seen traveling from longer to shorter wavelengths as the night progresses. This is reversed from what Riddle (2000) and Harrington et al. (2009) report.

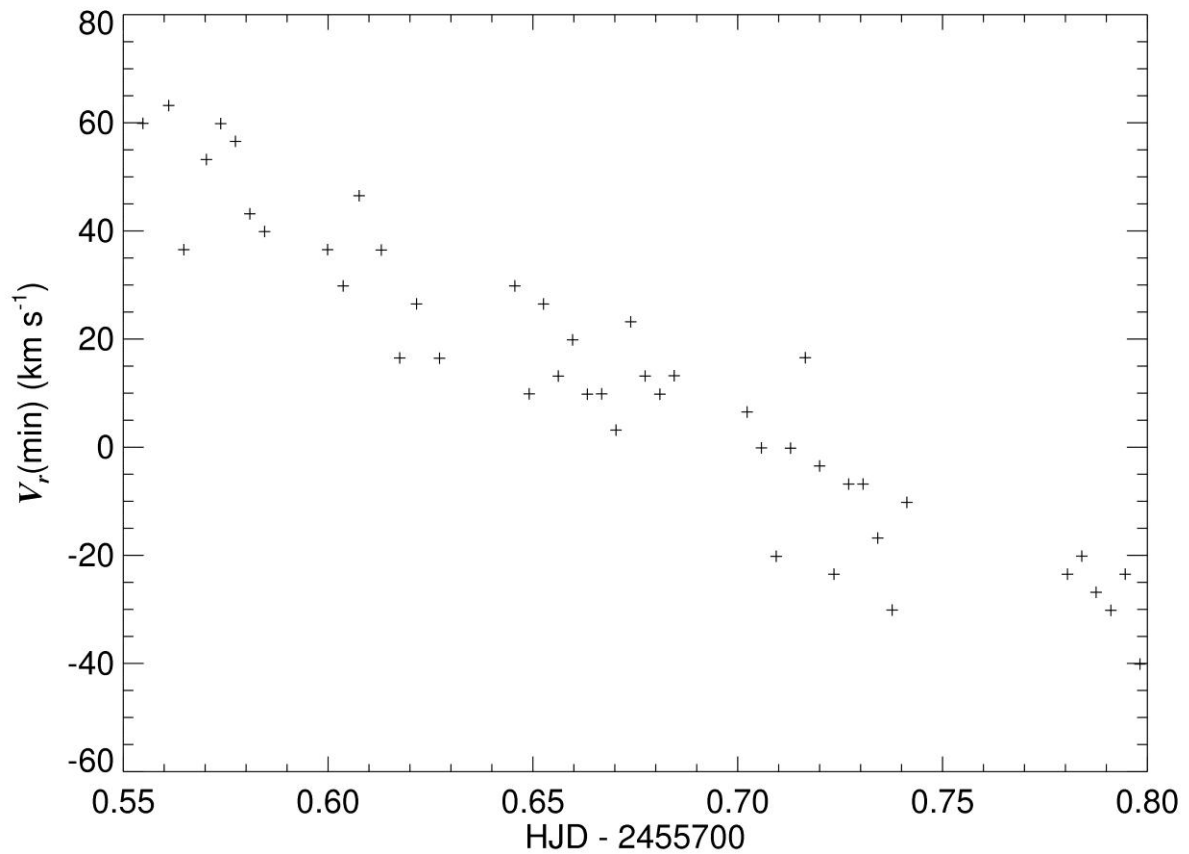


Figure 5.3: Radial Velocity of Line Profile Variability. This graph shows the general trend of the line profile variability from red to blue. The minimum of the profiles were found and then plotted in velocity space as they moved across the profile. V_{min} is the velocity of the minimum point in the profile. Notice that the change in the radial velocities equals about 90 km s^{-1} .

Table 5.1: Radial Velocity of α Vir Line Profiles. The following table contains the time of observations, the radial velocity measurement of the variability of the line profile, and the error of the measurement. The data corresponds to the points in Figure 5.3.

HJD- 2455700	V_{min} (km/s)	Error (km/s)
0.555	59.9	6.6
0.561	63.2	4.4
0.565	36.5	16.9
0.570	53.2	4.5
0.574	59.9	8.3
0.577	56.6	6.3
0.581	43.2	9.0
0.584	39.9	12.9
0.600	36.5	15.1
0.604	29.8	8.9
0.608	46.5	8.2
0.613	36.5	6.3
0.618	16.5	9.0
0.622	26.5	6.2
0.627	16.5	14.0
0.646	29.8	12.7
0.649	9.9	6.6
0.653	26.5	1.9
0.656	13.2	11.5
0.660	19.9	5.8
0.663	9.8	10.4
0.667	9.9	2.6
0.670	3.2	15.3
0.674	23.2	9.7
0.677	13.2	15.9
0.681	9.8	10.4
0.684	13.2	4.5
0.702	6.5	6.3
0.706	-0.1	14.3
0.709	-20.2	9.9
0.713	-0.2	9.6
0.717	16.6	31.1
0.720	-3.5	26.1
0.723	-23.5	13.9
0.727	-6.8	10.2
0.731	-6.8	10.2
0.734	-16.8	4.4
0.738	-30.1	9.9
0.741	-10.2	2.6

0.780	-23.5	8.1
0.784	-20.1	5.8
0.788	-26.8	11.5
0.791	-30.2	12.7
0.795	-23.5	8.1
0.798	-40.1	11.6

6. CONCLUSIONS

The final take away from all of this is that we are now capable of doing some interesting things with the newest instruments at HLCO. While hopes for a quickly interchangeable spectrograph might not have yet been realized, it is giving useable data on a regular basis. As was seen from the observations of α Vir, fairly accurate measurements can be made of the line profiles, even to the point of being able to detect a secondary spectrum from only one night of data. The non-radial pulsations of α Vir can also be seen in the Si III 4552, 4567, and 4574 Å features, showing that we have attained a high enough SNR to pick out interesting features. While true that this is a bright, well known star, and the equipment is not being pushed, the true value of these measurements is not to show the limits, but rather to show some of the capabilities of our new spectrograph. In this endeavor the measurements do quite well.

The other purpose of this study was to give future researchers a good background on the operation of the spectrograph, as well as ways to avoid some of the headaches that were encountered early on. Only time will tell if this study has been successful in its endeavors.

References

- Gray, D. F. 2005, *The Observation and Analysis of Stellar Photospheres* (Cambridge: Cambridge Univ. Press)
- Harrington, D., Koenigsberger, G., Moreno, E., & Kuhn, J. 2009, *ApJ*, **704**, 813
- Lanz, T., & Hubeny, I. 2007, *ApJS*, **169**, 83
- Riddle, R. 2000, Ph.D. dissertation (Atlanta: Georgia State University)
- Rodriguez-Merino, L. H., Chavez, M., Bertone, E., & Buzzoni, A. 2005, *ApJ*, **626**, 411
- Richardson, N. D., Morrison, N. D., Kryukova, E. E., & Adelman, S. J. 2011, *AJ*, **141**, 1
- Takeda, Y., Sato, B., & Murata, D. 2008, *PASJ*, **60**, 781

Appendix

A. Users Guide

A.1 Telescope Start-Up

1. Plug in the dome slit control and open the dome slit, adjust the lower slit as needed for object. Once finished unplug. (The plug will not rotate with the dome!)
2. Plug in the computer and telescope power strips and begin to boot the computers.
3. Turn on power boxes for the telescope and mount.
4. Remove guide scope eyepiece and objective lens covers. (*Important to do this step first so as not to risk damage to the primary mirror!*)
5. Remove objective cover of 20 inch.

Note: When slewing always be aware of the scope orientation. The telescope can, in some instances, point lower than horizon, and this is not good for the primary mirror!

Hitting any button on the paddle will pause the slew. DON'T LET THE TELESCOPE POINT DOWN!!!

6. If the telescope was properly parked the last time it was used (as it should always be) the following is the procedure to sync the telescope to a calibration star:
 - a. Select the following available option in this sequence: object -> star -> NEXT, PREV. (until you find your star) -> select GOTO, the scope will now slew to the selected star.
 - b. Center the star in the 20 inch telescope. The adjustments to the slew rate are found by pressing the \pm button on the hand paddle and then changing the speed using the PREV. (<) and NEXT. (>) buttons.
 - c. Once the star is centered select the NEXT (>) button.

- d. Hit #1 on the paddle.
7. The telescope is now synced.

A.2 Using the Spectrograph

Notes

- It is helpful to set up during daylight hours for several reasons. With a good solar spectrum atlas you can easily figure out where in the spectra you are looking. It is also handy to get your bias and dark frames out of the way early, and to make certain of all focus and collimation adjustments.
- When mounting the spectrograph onto the telescope, be sure you back-screw for a turn or two so as not to cross thread the adapter in the camera or the scope.
- The CCD will need to be aligned such that the spectral dispersion taken runs across the screen horizontally. A few minutes might be required to find the proper orientation.
- The power cord for the comp lamp is placed under unnecessary stress if left plugged in for extended periods of time. It is wise to plug and unplug the cord as needed for comp lamp exposures.
- All of the power bricks are marked for their intended use on the brick.

A.2.1. To Connect the ST-8 to the Computer

1. Make certain Windows is open on the computer before proceeding.
2. Connect the Power and one of the USB cables to the CCD.
3. Once at the computer follow the following sequence:
 - a. A Windows wizard pop-up will appear saying that the computer has found hardware; chose to not get driver online

- b. Install from list (don't search for manual driver, it should show it)
- c. The highlighted selected driver should be fine, hit next
- d. Select finish. (Should an error occur, one should select sbigulder found using the following path C:\Program files\SBIG\Driver Checker\SBIG Driver. This will work to sync the camera.)
- e. You are now ready to open Maxim DL

-Note: Before you disconnect the camera, be sure to turn off the cooler! Also every time the camera is disconnected it will need to be reconnected as above.

A.2.2. Maxim DL

1. Select camera control found in the view menu. (Alternatively use the camera Icon).
2. Under the camera tab click on select camera and chose Universal SBIG from the list.
3. Click on the connect button.
4. To turn cooling fans on from control window:
 - a. Under Camera 1 click on cooler button
 - b. Set temperature (can be up to 30° C below the ambient temperature)
 - c. Select ok, then turn the coolers on by clicking on the “on” button in the cooler section.
 - d. Wait at least 15 minutes for the camera to finish cooling before imaging.
5. To image go to expose tab.

A.2.3. Guide Camera

1. Attach the power, S-video, and control paddle cords to the camera.
2. Slot the camera into the eyepiece holder nearest to the telescope. See Figure A.1.

3. At the computer there is a USB device with audio/visual cables attached to it. This is connected to the S-video cable. Insert it into the front of the computer.
4. The program to run the guide camera is the VCL player. It is labeled guidecamera and is the icon with a traffic cone. Simply open this program and the images from the camera should appear with the text dshow:// at the bottom. If the image does not appear to be refreshing, make certain that the freeze button on the camera hand paddle is not depressed. (If it is depressed, then there will be a red light by FRZ.)
5. The refresh rate for the guide camera is determined by its hand paddle; adjust it as needed for the target which is being viewed. The gain and the refresh time might both need to be adjusted. Slower refresh times with higher gain are preferable for dimmer targets.

Note

- A known problem with the current guide camera is that it can overload. Simply powering the guide camera down and restarting it has cleared this issue with no further occurrence in a given night.



Figure A.1: A View of the Camera Positions. Note that the guide camera is to the right, nearest the telescope, and the ST-8 is located in the left position.

A.3. Prior to Observing

1. Make certain that the following programs are open on the computer:
 - a. RCOS TCC- this is the control for the focus of the telescope. While looking at the image from the guide camera make the image of the star as small as possible.
 - b. Pulse Guide v1.37- this is the control for fine guiding. Based on the image from the guide camera, use this control to keep the star centered on the slit. To connect simply select “connect.” Once connected go to the guide/slew tab for guiding.
 - c. VCL- for the guide camera.

- d. Maxim DL- for imaging.
2. Make certain that you have the projector for taking flat field images. It is stored in the electronics room under the desk.
3. Make certain that you have the desired grating and tilt. This is best checked by taking a solar spectrum and using a solar atlas to identify features near the waveband you wish to view.
4. To focus the spectrograph will require you to image the comp lamp. The simplest procedure is the following:
 - a. Turn on the lamp and place it in the path of the light. See Figure A.2 for the positions in and out of the path.
 - b. In Maxim DL chose frame type “light” and chose to continuously expose for enough time that the lines are bright, but that the CCD is not saturated.
 - c. Open the access panel to the collimator and using your finger turn the collimator. Note that both nylon screws need to be loosened. See Figures A.3 and A.4.
 - d. Check to see that the lines decrease in width. The lines need to be as narrow as possible. This will take some time.
 - e. Once satisfied, tighten the nylon set screws and replace the cover. One must replace the cover before taking a comp as stray light will ruin any spectra taken.
 - f. Always make sure to turn off and move the comp lamp out of the optical path once finished.
 - g. The final thing to finish the set up is to adjust the main mirror. This adjustment insures that the image of the slit will be across the center of the CCD. To do this, find the screw attached to the main mirror, Figure A.5. Loosen this screw only enough to

allow for it to slide up and down in its slot. {DON'T COMPLETELY UNSCREW IT!}

- h. Adjust the screw up or down until the image of the slit runs across the center of the CCD. Failure to do this can result in a doublet chromatism feature in your data.

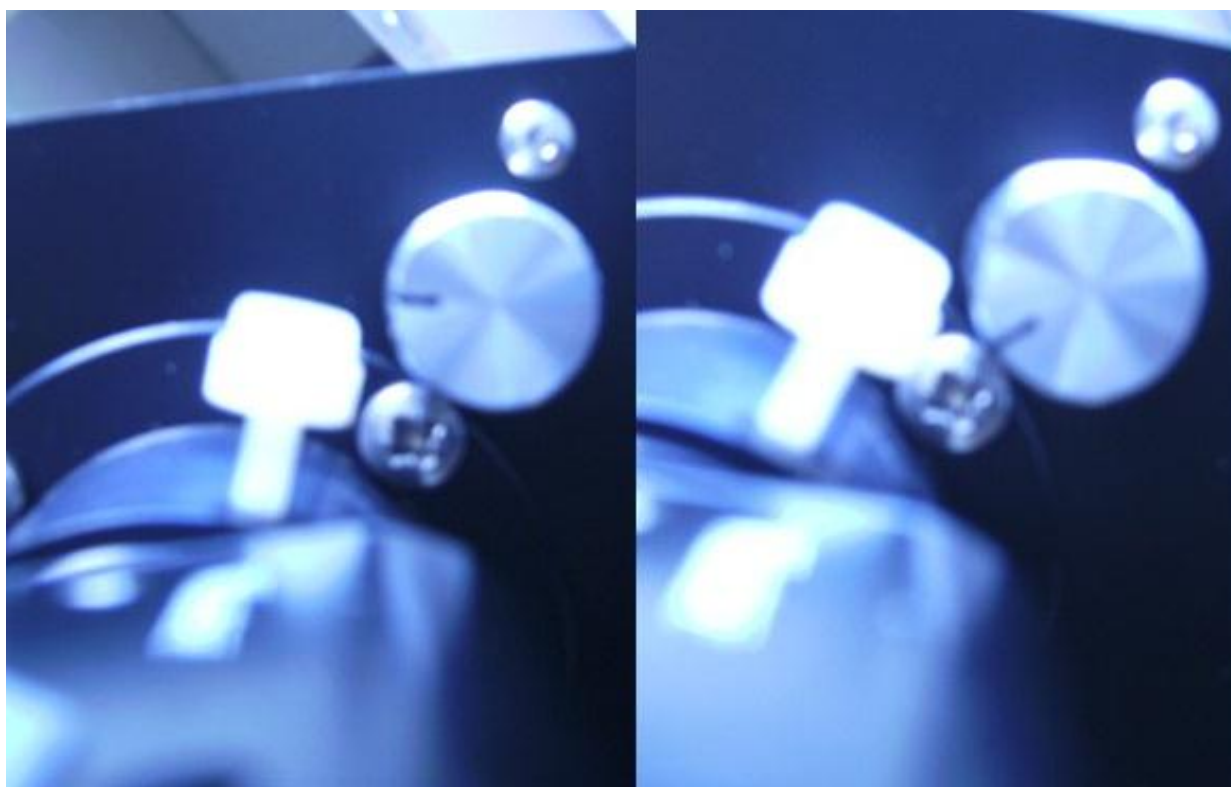


Figure A.2: Neon lamp configuration. A photo of the lamp removed from the optical path (left), and placed in the optical path (right). Note the difference in position of the dark line on the knob.

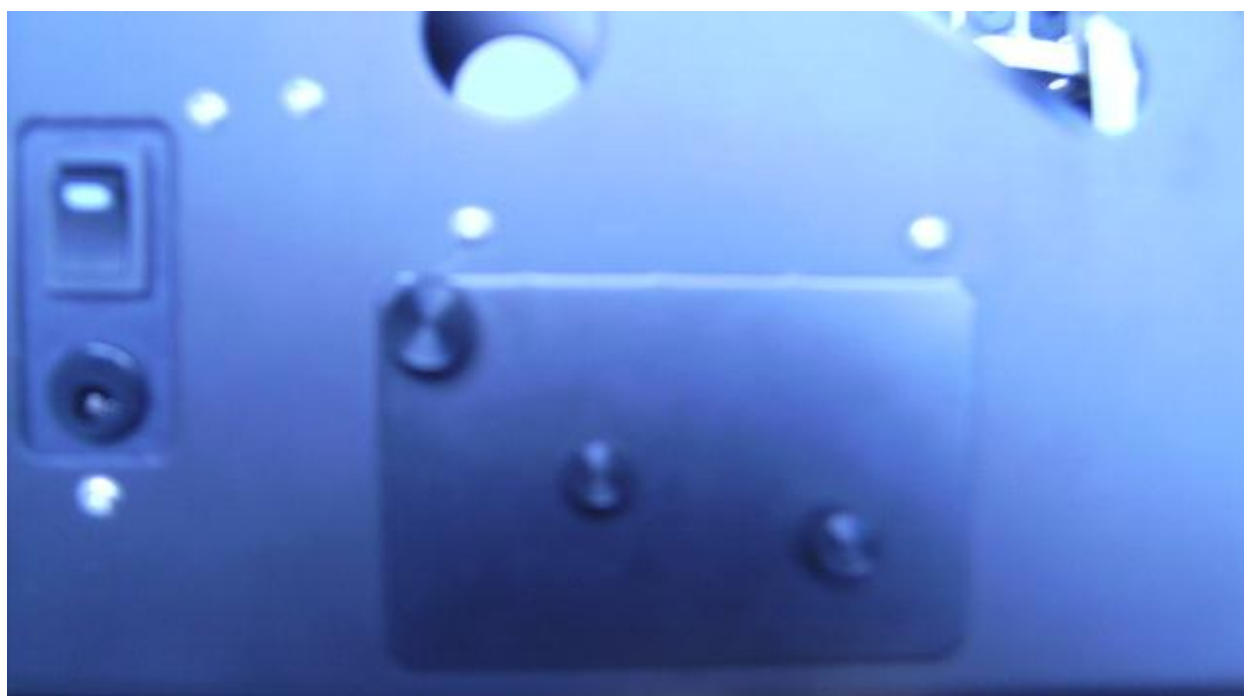


Figure A.3 Collimator access panel.



Figure A.4 Collimator adjustment.

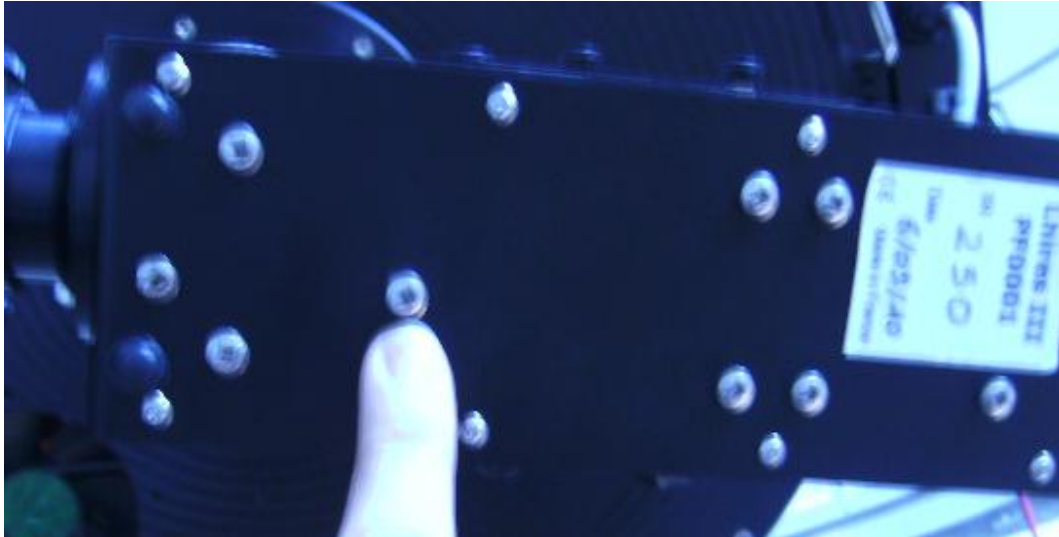


Figure A.5: The Main Mirror Adjustment Screw.

Notes:

- Make certain to leave sufficient time before you anticipate observing to be certain that the spectrograph is focused via the collimator. This can be a lengthy process.
- Any change in the tilt of the grating, or changing the grating itself requires refocusing of the collimator.
- Leave roughly fifteen minutes for fine adjustment of the collimator, for the most precise data collection, after adjusting the grating or tilt.
- The main mirror will only need to be adjusted if the grating is changed.

A.4. Observing Procedure

1. To obtain bias frames, select the autosave option in the expose tab and select type bias and desired number of bias frames from menu. Make certain of proper naming and save path. Ten bias frames are sufficient, and this will only need to be done once per observing run.
2. To obtain images of spectra and comp lamp spectra:
 - a. Select the single exposure option.
 - b. Make certain that the type of frame is “light.”

- c. Set your exposure time in seconds.
- d. Select start to begin imaging.
- e. While imaging, be certain to keep the object located on the slit the entire exposure.

This requires one to guide by the following manual procedure:

- i. While looking at the VCL guidecam player the object should be located on the slit. It is sometime possible to see the slit across the object. More often than not it will not be possible. The best thing to do is to affix a Post-It note along the slit as a point of reference. This is best done by using the projector, or during daylight hours to illuminate the mirror and locate the slit in the guide camera field of view. Using a corner of the Post-It as a reference will allow you to keep the object in a fixed point during observing.
 - ii. Once the slit has been marked the star must be placed upon the slit. Using the Pulse Guide v1.37 program use the N, S, E, and W buttons to keep the object in the same point. It will take some time on the part of the user to become accustomed to the direction in guide camera which corresponds to a direction button in Pulse Guide. These will also change some depending upon the position of various objects in the sky relative to the telescope placement about the pier.
- f. For strong emission features, make certain that the counts for the feature are several thousand, compared to the rest of the spectra which should be in the hundreds, and over the background which should be in the low hundreds.

- g. For a comp lamp, make certain that the lamp is on and in the optical path. See Figure A.1. These exposures will need to be done immediately before or after any spectra taken.
- h. Always make certain to turn off and move the comp lamp out of the optical path once done.
- i. When saving these images, you **must manually add** “.fits” to the end of the name so as to get a .fits file.
- j. If you would like to change anything in the fits header of subsequent images:
 - i. Go to the File menu of Maxim DL
 - ii. Select settings
 - iii. Once the settings menu is up select the Fits Header tab
 - iv. After making the desired change in any field click the set button.
 - v. Once all desired changes have been made exit the setting menu. The changes will be applied to any image taken after the change has been made.

Note: If one would like a quick look at the cross section of the spectra while in Maxim DL follow these steps:

- a. Select the View menu.
- b. Select the Graph Window from the drop down box.
- c. In the pop-up box select either horizontal box, or horizontal line. (For this to work the spectra must be nearly horizontal on the CCD, the horizontal box option is slightly more forgiving about the orientation.) Do not close the pop-up menu.

- d. Go to the image in Maxim DL and click and drag over the area you wish to view. If the Horizontal Box option is used the bottom of the box will be placed atop the spectra.
 - e. A 2-D image of the spectral emission and/or absorption should be visible in the pop-up menu.
 - f. If the Horizontal Box option is used once the Graph Window is closed, then the subframe must be resized. If it is not, then subsequent images will only have the area within the box recorded. To resize the image go the expose tab in the camera control. The button in the far right of the Subframe box needs to be selected. The pixels of the subframe size should return to the size of the image. It should be 1530 x 1020, or whatever fraction of that pixel size your binning allows.
3. Flats will need to be taken before any change is made to the grating or the tilt. If no changes are made, they can be taken at the end of the night. It is recommended that three flats be taken each time flats are required. One minute flats are usually sufficient for moderate exposures. This will give counts which average around 2000. To take a flat:
 - a. Select the autosave feature.
 - b. Choose frame type "flat."
 - c. Choose your exposure time. A one minute exposure should be sufficient.
 - d. Select the number of flats you wish to take.
 - e. Make certain of proper naming and save path.
 - f. Move the dome such that the telescope is pointed at the interior of the dome.

- g. Using the projector illuminate the interior of the dome where the telescope is pointed.
Make certain that the entire objective is pointed at an illuminated portion of the wall.
 - h. Begin exposing your flat field frames.
4. Dark frames will be done at the beginning or end of the night but only once per observing run. Usually five darks will suffice. To get a dark frame:
- a. Select the autosave feature.
 - b. Choose frame type “dark.”
 - c. Choose your exposure time. Make certain that your dark frames are at least as long as your longest exposure of the night.
 - d. Select the number of darks you wish to take.
 - e. Make certain of proper naming and save path.
 - f. Begin exposing your dark frames.

A.5 Closing Down

1. Once all exposures have been completed, begin warming-up the CCD. To do so go to the set-up tab in Maxim DL select the warm-up option in the cooler controls.
2. While the CCD is warming up all programs other than Maxim DL can be closed down.
 - a. Do not close Maxim DL until the CCD has been properly warmed and disconnected.
3. Once the other programs are shut down the USB for the guide camera can be removed from the computer.
4. To park the telescope:
 - a. Hit the Menu button until the main menu screen appears.
 - b. Select set up option from the main menu.
 - c. Select park option #3.

- d. Once the telescope is done slewing the power can be turned off at the two power supplies.
 - e. When replacing the covers for the telescope optics, care should be taken that the first cover replaced is the primary cover so as not to drop anything on it and risk damage.
5. To close the dome;
- a. The dome slit should point northeast. This should be easy as it is the only place at which to lower the slit.
 - b. Once the slit has been lowered completely make certain that the slit control is unplugged.
 - c. Make certain that any windows opened, or fans turned on during the observing run have been closed or shut down.
6. At the telescope make certain that all wires going to the guide camera have been removed. This should include the power, the S-video, and the hand paddle cables.
7. Once the chip has been warmed to ambient temperature it is safe to disconnect the CCD from the computer.
- a. Go to the camera control in Maxim DL and select the option to turn off the coolers.
 - b. Then disconnect the CCD by selecting the disconnect option.
 - c. You can now close Maxim DL and begin to shut down the computers.
8. Back at the telescope remove the power cable and the USB cable from the CCD. If the spectrograph is remaining on the telescope then it can be left as is.
9. If the spectrograph is to be removed:
- a. Remove the CCD and the guide camera and replace the eyepiece covers.

- b. When unscrewing the spectrograph be certain that the black rings on the telescope are not coming unscrewed. The only thing that should be moving is the aluminum plate attached to the spectrograph. BE CAREFUL TO MAINTAIN A GOOD HOLD THE ENTIRE TIME WHILE UNSCREWING! The threads are fine and the spectrograph will come free quickly.
 - c. Replace all eyepiece covers on the spectrograph and return it to the carry case.
 - d. Screw the 2 inch eyepiece holder onto the telescope and place an eyepiece cover on it.
 - e. Remove all equipment to the electronics room.
10. Make certain that everything is shut down and then unplug the power strips.
11. Double check that the dome is closed and unplugged.
12. Turn off the lights and make certain that the door shuts.

B. Atlas of Neon Lines

Table B.1 is intended to give the user a general idea of the lines in a particular wavelength range which are of use for comparison spectra and subsequent wavelength calibration. It is not exhaustive, nor will all of the lines be seen. These are just the most likely to aid in identification of the neon comparison lamp for wavelength calibration. In the blue there are few to no lines visible, and it is suggested that in the future the Th-Ar lamp, which was used with the MTT, be utilized for blue wavelength calibrations.

Table B.1 Known Ne Lines.

Wavelength (Å)
5748.2985
5764.4188
5804.4496
5820.1558
5852.4878
5881.895
5944.8342
5975.534
6029.9971
6074.3377
6096.1631
6128.4499
6143.0626
6163.5939
6217.2812
6266.495
6304.789
6334.4278
6382.9917
6402.246
6506.5281
6532.8822
6598.9529
6678.2764
6717.043
6929.4673
7024.0504
7032.4131

7173.9381
7245.1666
7438.899
7488.8712
7535.7739
8136.4057